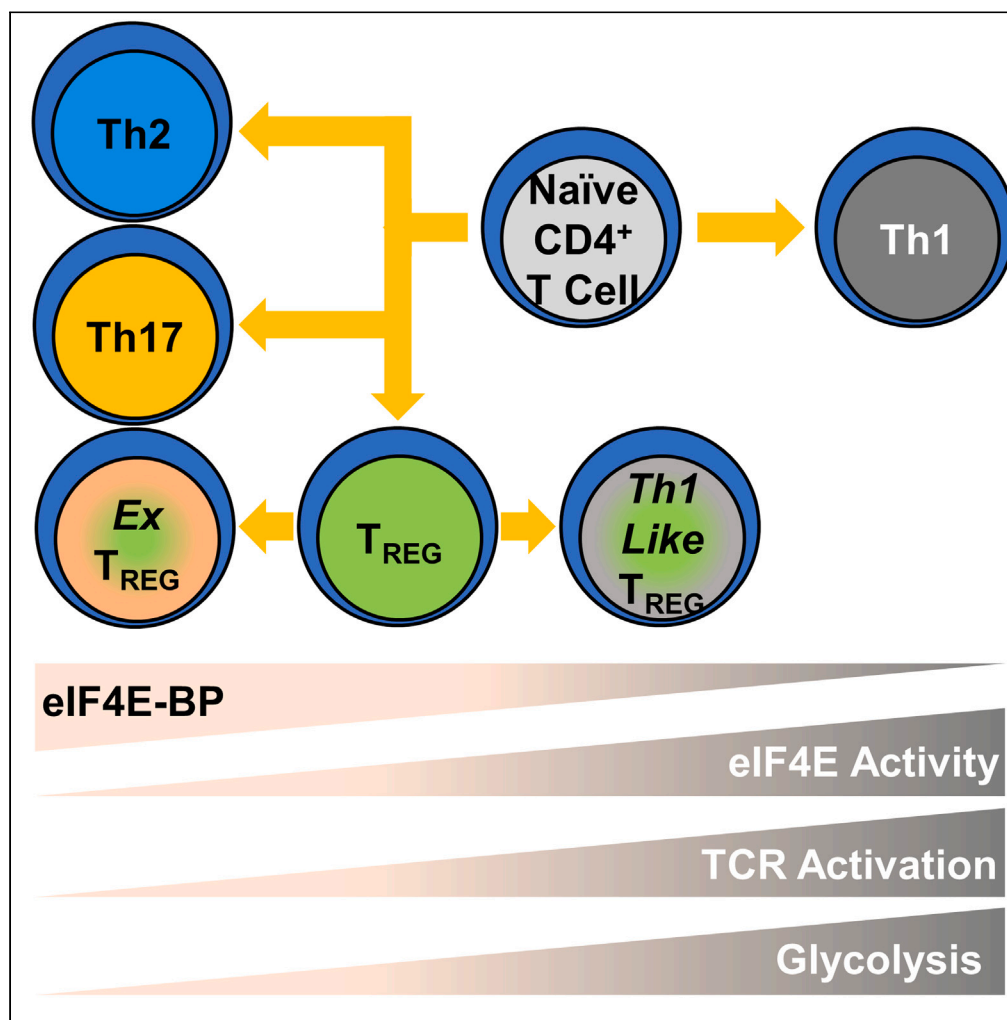


Article

The eIF4EBP-eIF4E axis regulates CD4⁺ T cell differentiation through modulation of T cell activation and metabolism



Roman Istomine,
Tho-Alfakar Al-
Aubodah,
Fernando Alvarez,
Jacob A. Smith,
Carston Wagner,
Ciriaco A. Piccirillo

ciro.piccirillo@mcgill.ca

Highlights

The eIF4E-BP axis influences T cell activation and differentiation

Increased eIF4E activity in T cells promotes IFN γ secretion *in vitro* and *in vivo*

Absence of eIF4E-binding proteins drives increased glycolytic activity



Article

The eIF4EBP-eIF4E axis regulates CD4⁺ T cell differentiation through modulation of T cell activation and metabolism

Roman Istomine,^{1,2,3} Tho-Alfakar Al-Aubodah,^{1,2,3} Fernando Alvarez,^{1,2,3} Jacob A. Smith,⁴ Carston Wagner,⁴ and Ciriaco A. Piccirillo^{1,2,3,5,*}

SUMMARY

CD4⁺ T cells are critical for adaptive immunity, differentiating into distinct effector and regulatory subsets. Although the transcriptional programs underlying their differentiation are known, recent research has highlighted the importance of mRNA translation in determining protein abundance. We previously conducted genome-wide analysis of translation in CD4⁺ T cells revealing distinct translational signatures distinguishing these subsets, identifying eIF4E as a central differentially translated transcript. As eIF4E is vital for eukaryotic translation, we examined how altered eIF4E activity affected T cell function using mice lacking eIF4E-binding proteins (BP^{-/-}). BP^{-/-} effector T cells showed elevated Th1 responses *ex vivo* and upon viral challenge with enhanced Th1 differentiation observed *in vitro*. This was accompanied by increased TCR activation and elevated glycolytic activity. This study highlights how regulating T cell-intrinsic eIF4E activity can influence T cell activation and differentiation, suggesting the eIF4EBP-eIF4E axis as a potential therapeutic target for controlling aberrant T cell responses.

INTRODUCTION

CD4⁺ T effector (T_{EFF}) cells are central mediators of the adaptive immune response, with distinct T helper cell (Th) subsets arising depending on the nature and location of immune challenges like infections. Key among these subsets are IFN γ -secreting Th1 cells, IL-4-secreting Th2 cells, and IL-17A-secreting Th17 cells, whose transcriptional programs are driven by the lineage-defining master transcription factors T-bet, GATA3, and ROR γ t, respectively.^{2,3} Despite the essential nature of T_{EFF} cells in conferring immune protection to the host, a fine balance must be maintained to ensure appropriate and timely T cell differentiation, prevent tissue damage from excessive inflammation, and limit aberrant responses to self-antigens. This balance is maintained by CD4⁺ regulatory T (T_{REG}) cells, constitutively expressing the master transcription factor Foxp3, which are crucial in resolving inflammation and maintaining tolerance to self in both mice and humans.^{4–6} To ensure an appropriate and timely immune response is mounted, a finely regulated balance of T_{EFF} and T_{REG} cell responses and their adaptation to evolving inflammatory signals is essential to their function.^{7–9} During infections, the expansion and differentiation of inflammatory T_{EFF} subsets in early phases is permitted, while T_{REG} cell function is harnessed in later stages to suppress anti-pathogen immunity, limit inflammation, and facilitate tissue recovery upon pathogen clearance.^{10–12} The integration of extracellular signals including alarmins, cytokines, and metabolic cues drives the development of CD4⁺ T cell subsets with divergent effector profiles, enabling context-dependent responses *in situ*.

While the transcriptional profiling of T_{EFF} and T_{REG} cells has identified distinct gene signatures defining their function, it was shown that the rate of mRNA translation can affect the proteome to the same extent as transcription and thus greatly impact T cell function.^{13,14} A growing body of evidence indicates a complex network of translational control mechanisms including the modification of mRNA untranslated regions, miRNA interference, and RNA-binding proteins capable of altering protein expression and effector function within immune cells.^{15–17} Previously, we conducted the first genome-wide screen for differentially translated mRNA transcripts in both T_{REG} and T_{EFF} cells to determine whether these translational control mechanisms could affect T cell function.¹⁸ We identified unique translomes distinguishing T_{REG} and T_{EFF} cells, capable of influencing the proteomes of these cells independent of transcription.

¹Department of Microbiology and Immunology, McGill University, Montréal, QC H3A 2B4, Canada

²Program in Infectious Diseases and Immunology in Global Health, Centre for Translational Biology, Research Institute of the McGill University Health Centre, Montréal, QC H4A 3J1, Canada

³Centre of Excellence in Translational Immunology (CETI), Montréal, QC H4A 3J1, Canada

⁴Department of Medicinal Chemistry, University of Minnesota, Minneapolis, MN 55455, USA

⁵Lead contact

*Correspondence:

ciro.piccirillo@mcgill.ca

<https://doi.org/10.1016/j.isci.2023.106683>



The mRNA encoding the eukaryotic translation initiation factor, eIF4E, is preferentially translated in activated T_{EFF} cells compared to T_{REG} cells, and accounts for approximately 10% of the transcriptome differences that were observed between activated T_{EFF} and T_{REG} cells.¹⁸ eIF4E is a central regulator of eukaryotic translation. eIF4E binds to the 5' cap of mRNA, as well as eIF4G to assemble the eIF4F translation initiation complex, necessary for the recruitment of ribosomes.¹⁹ eIF4E has been widely studied for its role as an oncogene, with eIF4E overexpression leading to the development of various cancer cell types.^{20–24} The expression and activity of eIF4E is tightly regulated through both transcriptional and post-transcriptional mechanism, including protein interactions.^{25,26} One such group of regulators are the family of eIF4E-binding proteins, eIF4EBP 1, 2, and 3 which bind and sequester eIF4E.^{27,28} While little is known about eIF4EBP3 activity, eIF4EBP1 and 2 expression has been identified in both human and murine CD4⁺ T cells.²⁹ Activation of the mammalian target of rapamycin (mTOR) complex results in the phosphorylation of these binding proteins, liberating eIF4E to act within a cell. Blockade of eIF4EBP phosphorylation directly impacts cellular translation through the sequestration of eIF4E.³⁰ eIF4EBP1 deficiency also impacted the localization of eIF4E to the cytoplasm.³¹ Meanwhile, overexpression of eIF4EBP1 blocked cell proliferation in several studies.^{29,32} In addition, we have previously reported how inhibition of eIF4E using a small molecule inhibitor impaired both T_{EFF} and T_{REG} cell proliferation.¹⁸ Thus, given the preferential translation of eIF4E mRNA observed in T_{EFF} cells, we sought to examine the role of eIF4E on the activation, differentiation, and function of CD4⁺ T cells.

The ability of eIF4E to bind the 5' cap of mRNAs has been shown to be directly linked to the presence of eIF4E-binding proteins, requiring the phosphorylation of eIF4EBPs for them to dissociate from eIF4E and allow translation to occur.^{33,34} Furthermore, knockdown of eIF4EBP1 and 2 was found to directly affect eIF4E activity through increased phosphorylation of eIF4E.³⁵ Thus, we made use of eIF4EBP1 and 2 double-deficient (BP^{-/-}) mice to examine how a lack of essential negative regulators of eIF4E, and ensuing eIF4E hyper-activity, could impact T cell functions *in vitro* and *in vivo*. We found that increased eIF4E activity afforded by a lack of eIF4EBP1 and 2 in CD4⁺ T_{EFF} cells conferred an increased sensitivity to T cell activation signals and skewed their differentiation toward a Th1 phenotype at baseline as well as during lung viral infection and gut inflammation. Proteomic analysis of BP^{-/-} and wild-type (WT) CD4⁺ T cells revealed differential expression of several proteins involved in cell activation and proliferation, including genes involved in regulating T cell metabolic processes. Furthermore, increased eIF4E activity altered the metabolic profile of BP^{-/-} T_{EFF} cells by increasing glucose uptake and glycolytic activity. Thus, the regulation of eIF4E activity in T cells contributes to their ability to differentiate into different Th cell subset lineages, in part through control of their activation and metabolic activity. We identify the eIF4EBP-eIF4E axis as potential therapeutic target for the control of T_{EFF} cell function through regulation of their inflammatory capacity.

RESULTS

The lack of eIF4E-binding proteins to regulate eIF4E activity in T cells exacerbates Th1 responses during viral lung infection

Previously, we showed that the mRNA encoding eIF4E was differentially translated in CD4⁺ T cell subsets and underlies many functional characteristics of T_{EFF} and T_{REG} cells, including their responsiveness to T cell receptor (TCR)-induced proliferation and cytokine production.¹⁸ We examined whether a dysregulation in eIF4E activity in T cells could have a direct impact on the nature, magnitude, and progression of the adaptive immune response. We first examined if there was a baseline difference in T_{EFF} cell function in BP^{-/-} mice, where eIF4E is hyper-active due to a loss of control by eIF4EBP1 and 2.^{36,37} Although there was no significant difference in the ability of splenic T_{EFF} cells extracted to secrete IFN γ upon PMA and ionomycin stimulation, the inflammatory capacity of BP^{-/-} T_{EFF} cells was increased within the colon, with a higher proportion of BP^{-/-} T_{EFF} cells secreting IFN γ , a prototypic signature cytokine of Th1 cells (Figure 1A). Surprisingly, this bias in cytokine secretion was limited to Th1 responses as BP^{-/-} T_{EFF} cells showed a decrease in the frequency of both IL-4-secreting Th2 and IL-17-secreting Th17 cells (Figure 1B). This specific Th1 bias in unchallenged mice led us to investigate whether the increased eIF4E activity in BP^{-/-} T cells could also enhance Th1 responses upon pathogen challenge. To this end, we employed an H1N1 *Influenza A* infection model which is characterized by robust Th1 differentiation of CD4⁺ T_{EFF} cells and infiltration of CD8⁺ CTLs within the lungs of infected mice, central components for effective antiviral immune responses.^{38,39} Importantly, excessive T cell responses during viral infection can lead to exacerbated immunopathology and tissue damage.^{40–42} Mice were infected with a sublethal (1/4 LD₅₀) dose of *Influenza A* to determine if the basal Th1 bias in BP^{-/-} mice would result in an exacerbated Th1 response during infection leading to greater weight loss and a delayed recovery period. Infected BP^{-/-} mice failed to recover as indicated by the

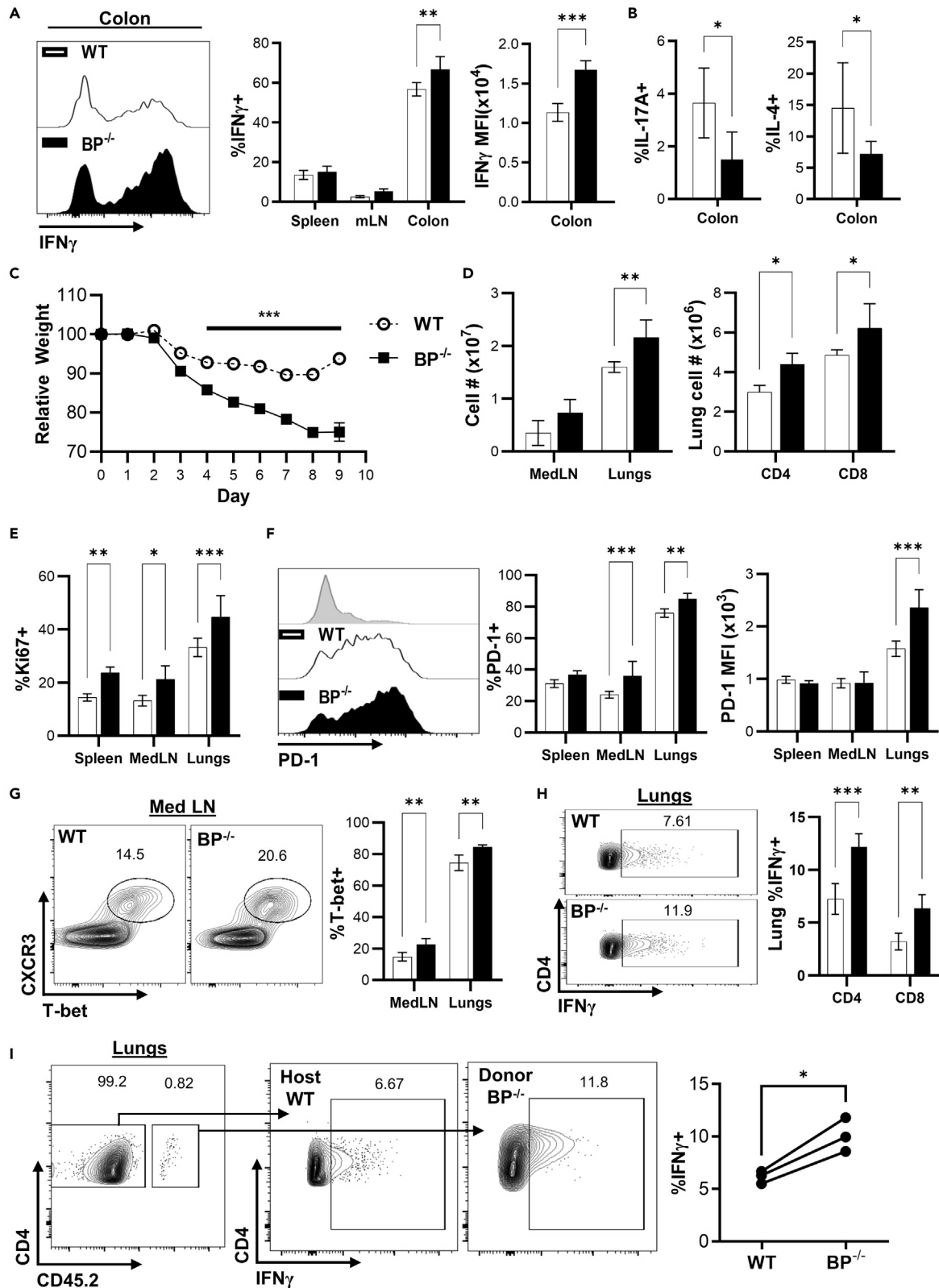


Figure 1. Lack of eIF4E regulation via the eIF4E-binding proteins enhances Th1 cell responses during viral infection

- (A) IFN γ expression was assessed in CD4⁺ T_{EFF} in WT and BP^{-/-} mice directly *ex vivo* (showing representative plot of 3 individual experiments, n = 3–4 per group).
- (B) IL-17A and IL-4 secretion assessed in the colons of WT and BP^{-/-} mice.
- (C) WT or BP^{-/-} mice (n = 5 per group, with 3 experimental repeats) were infected intranasally with 1/4 LD₅₀ dose of H1N1 influenza A virus. Relative weight loss curve shown from one representative experiment.
- (D) Total cell recovery from lungs, and mediastinal lymph nodes shown at day 9 post infection. CD4 and CD8 T cell counts recovered from the lungs of infected mice show increased T cell infiltration in BP^{-/-} mice.
- (E) A higher proportion of BP^{-/-} T_{EFF} cells are actively proliferating.
- (F) BP^{-/-} T_{EFF} cells express higher levels of PD-1 expression.
- (G) BP^{-/-} mice had a higher proportion of Th1 T_{EFF} as marked by increased frequencies of T-bet expressing cells.
- (H) The proportion of IFN γ -secreting T cells is elevated in BP^{-/-} mice. Cytokine secretion was measured within CD4⁺ and CD8⁺ T cells following PMA/Ionomycin/Monensin stimulation for 3 h.
- (I) 8 million CD45.2 BP^{-/-} CD4⁺ cells were intravenously injected into CD45.1 WT mice prior to influenza infection. Donor CD45.2 BP^{-/-} T_{EFF} cells showed increased IFN γ secretion compared to host CD45.1 WT T_{EFF} cells. (n = 3 per group). Paired t test. All cytokine secretion data are from cells treated with PMA, Ionomycin, and Golgi-Stop for 3 h. Data are represented as mean \pm SD. Statistical significance was determined using a two-way ANOVA with Šidák correction unless otherwise indicated. * = p < 0.05, ** = p < 0.01, *** = p < 0.001.

augmented weight loss compared to WT controls, with experiments being terminated at 9 days post infection due to BP^{-/-} mice having reached clinical endpoint (sustained >20% weight loss). In contrast, WT mice showed signs of recovery from weight loss at this time point (Figure 1C). Infected BP^{-/-} mice also showed increased infiltration of CD4⁺ and CD8⁺ T cells in the lungs (Figure 1D), with CD4⁺ T_{EFF} cells displaying an increased frequency of actively proliferating cells, marked by Ki67 expression (Figure 1E). This increased activation was corroborated by elevated proportions of PD-1⁺ and PD-1 expression in lung-infiltrating BP^{-/-} T_{EFF} cells (Figure 1F). Furthermore, lung-infiltrating BP^{-/-} T_{EFF} cells also showed increased levels of Th1 differentiation, with a higher proportion of cells expressing the Th1 master transcription factor, T-bet (Figure 1G). Consequently, IFN γ secretion was elevated in BP^{-/-} lungs, with more CD4⁺ and CD8⁺ T cells secreting IFN γ (Figure 1H). As BP^{-/-} mice are globally deficient for eIF4EBP1/2 expression in all cell types, including antigen-presenting cells, we then transferred CD45.2⁺ BP^{-/-} CD4⁺ T cells into congenic CD45.1⁺ WT hosts and repeated this infection to directly assess the T cell-intrinsic role of eIF4EBP1/2 in the absence of any potential influence of these proteins on antigen-presenting cells. Donor BP^{-/-} T_{EFF} cells (CD45.2⁺) recovered within the lungs of infected mice, showed higher levels and frequencies of IFN γ -secreting T cells, compared to host WT T cells (CD45.1⁺) (Figure 1I). Thus, eIF4E hyper-activity in BP^{-/-} T_{EFF} cells directly promoted Th1 differentiation, in turn fueling antiviral Th1 immunity and reduced disease recovery during *Influenza A* infection.

Enhanced eIF4E activity in BP^{-/-} CD4⁺ T_{EFF} drives greater Th1 polarization *in vitro*

Our results showed that BP^{-/-} mice had skewed Th1 responses, while having diminished Th2 and Th17 cells *in vivo*. We then assessed whether the increased eIF4E activity in BP^{-/-} CD4⁺ T cells impacted their ability to polarize to different Th subset lineages *in vitro*. To this end, we differentiated fluorescence-activated cell sorting (FACS)-isolated Foxp3⁻ (GFP⁻) naive (CD62L⁺CD44⁻) CD4⁺ T cells toward different Th cell lineages using the requisite polarizing cytokines and examined their capacity to secrete the corresponding cytokines using PMA and ionomycin stimulation. Under Th2 polarizing conditions, BP^{-/-} T_{EFF} cells displayed a reduced potential for Th2 differentiation as the frequency of IL-4-secreting CD4⁺ T cells was reduced compared to WT counterparts (Figure 2A). Similarly, naive BP^{-/-} T cells activated under Th17 polarizing conditions (TGF- β and IL-6) showed a reduction in the proportions of IL-17⁺ CD4⁺ T cells compared to WT cells (Figure 2B). Furthermore, BP^{-/-} T cells showed impaired STAT3 signaling, essential for Th17 cell development, with a lower proportion of phospho-STAT3 expressing cells following treatment with IL-6 (Fig. S1A). Moreover, naive BP^{-/-} CD4⁺ T cells showed reduced expression of Foxp3 when polarized under iT_{REG} inducing conditions (TGF- β) (Figure 2C). Treating cells with a small molecule inhibitor of eIF4E activity (eIF4Ei-1) showed the opposite effect, indicating that the degree of eIF4E activity in CD4⁺ T cells influenced their ability to convert to an iT_{REG} phenotype (Figure S2A). Finally, we examined the potential for Th1 polarization by naive BP^{-/-} T cells using IL-12. BP^{-/-} T cells showed an increase in both the proportion of IFN γ secreting cells, as well as the level of IFN γ expression per cell (Figure 2D). However, STAT4 activity was unaffected with BP^{-/-} and WT T cells having equivalent phospho-STAT4 expression following IL-12 treatment (Figure S1B). In addition, inhibiting eIF4E activity using the eIF4Ei-10 small molecule reduced IFN γ secretion in T cells cultured in Th1 polarizing conditions (Figure S2B). Since eIF4E is known to be phosphorylated at Ser209 by MNK1/2, we also examined if phosphorylation of Ser209 was required for the increased Th1

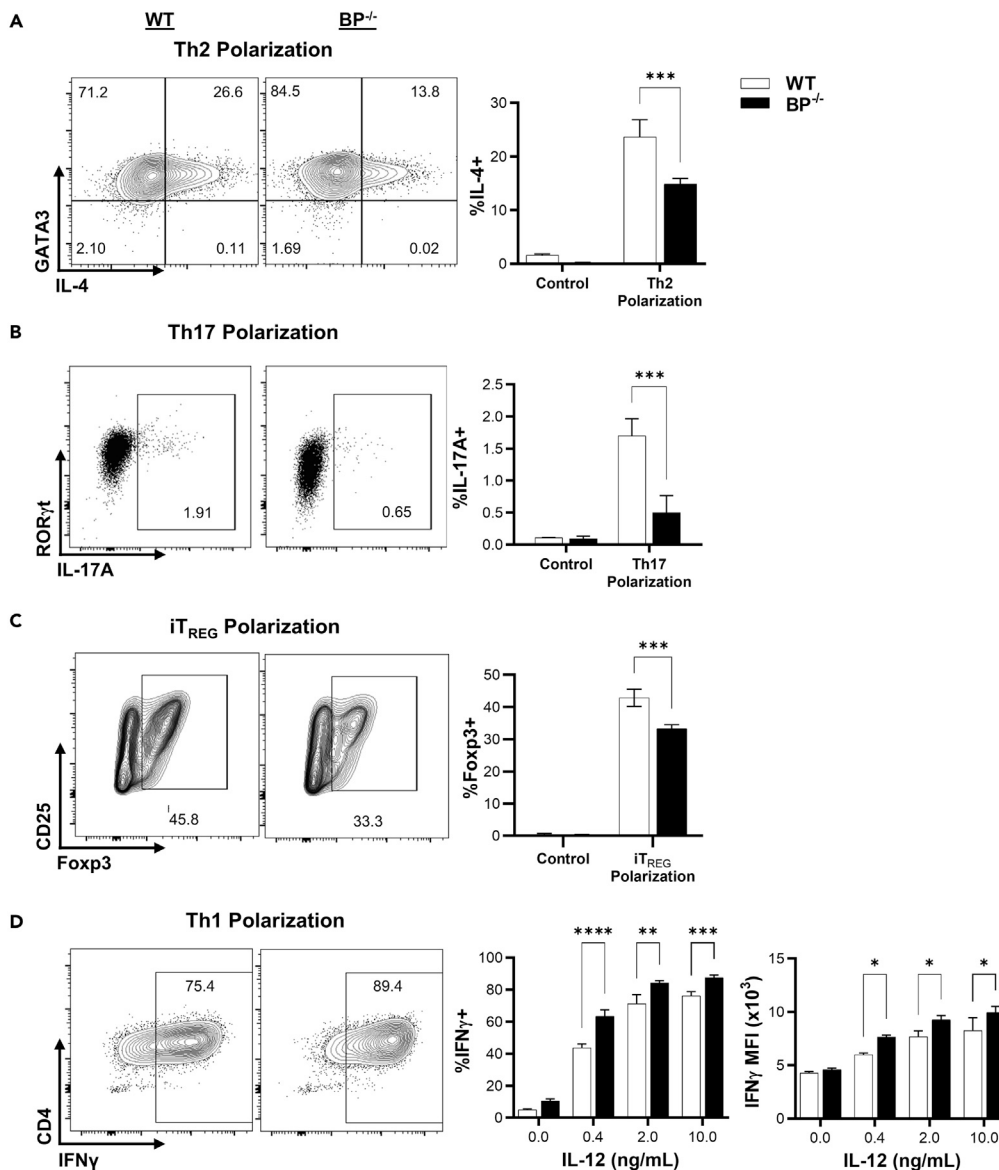


Figure 2. Increased eIF4E activity in $BP^{-/-}$ T_{EFF} cells skews cells to a Th1 phenotype *in vitro*

T_{EFF} cell polarizations were conducted using sorted T_{EFF} cells cultured with the indicated concentrations of polarizing cytokines.

(A) Naive $CD4^{+}$ T cells were polarized toward a Th2 phenotype in the presence of IL-4 (2 ng/mL) for 72 h.

(B) Naive $CD4^{+}$ T cells were polarized toward a Th17 phenotype in the presence of TGF- β (1 ng/mL) and IL-6 (10 ng/mL) for 72 h.

(C) Naive $CD4^{+}$ T cells were polarized in the presence of TGF- β (5 ng/mL) to an iT_{REG} phenotype for 72 h.

(D) Naive $CD4^{+}$ T cells were polarized in the presence of IL-12 at the indicated concentrations for 72 h. All cytokine secretion data are from cells treated with PMA, Ionomycin, and Golgi-Stop for 3 h. Showing representative plots from 1 of 3 individual experiments. Data are represented as mean \pm SD. Statistical significance was determined using a two-way ANOVA with Sidák correction. * = $p < 0.05$, ** = $p < 0.01$, *** = $p < 0.001$.

polarization in $BP^{-/-}$ $CD4^{+}$ T cells by inhibiting MNK1/2 activity.⁴³ T_{EFF} cells treated with a selective MNK1/2 inhibitor (eFT508), which is known to cause a dose-dependent decrease in eIF4E phosphorylation, showed a reduction in the proportion of both T-bet- and IFN γ -secreting cells (Figure S2C).⁴⁴ Altogether, enhanced eIF4E activity in $BP^{-/-}$ $CD4^{+}$ T cells skewed their differentiation toward a Th1 phenotype, corroborating our results observed in both naive and *Influenza A*-infected $BP^{-/-}$ mice.

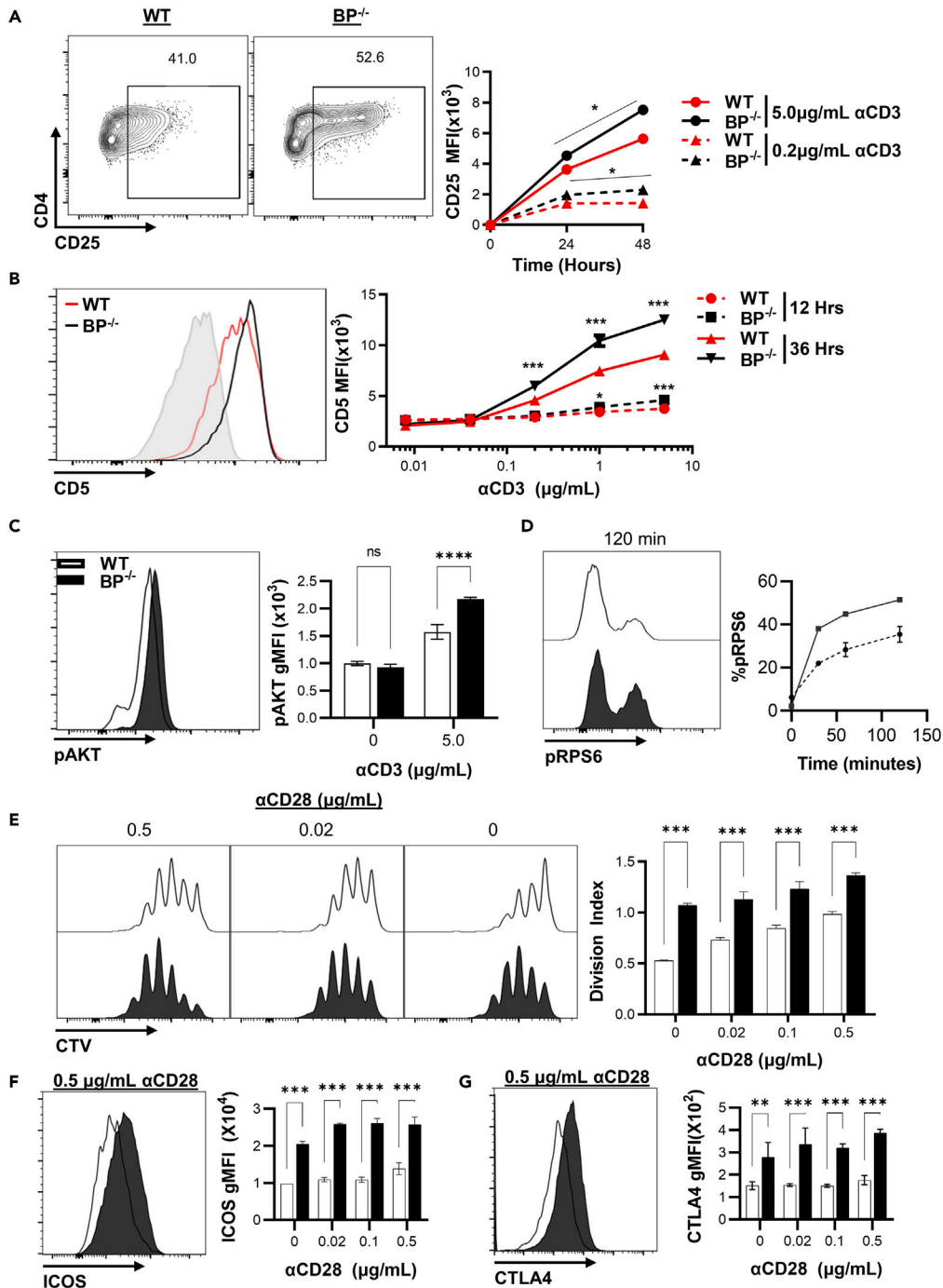


Figure 3. Enhanced eIF4E activity in BP^{-/-} T_{EFF} cells increases their sensitivity to TCR and co-stimulatory signals

(A) Representative plots of CD25 expression following TCR stimulation (48 h, 0.2 μg/mL αCD3). CD25 expression was assessed following at the indicated time points with sorted naive CD4⁺ T cells (CD62L⁺CD44⁻) being exposed to platebound TCR stimulation using the indicated concentrations of αCD3, with constant αCD28 (2 μg/mL).

(B) CD5 expression was measured at the indicated time points following platebound TCR stimulation.

(C) Assessment of phosphorylated AKT levels in naive CD4⁺ T cells activated for 2 h using platebound αCD3 (2 μg/mL) and αCD28 (2 μg/mL).

(D) Assessment of phosphorylated RPS6 expression in naive CD4⁺ T cells activated for up to 2 h using platebound αCD3 (2 μg/mL) and αCD28 (2 μg/mL).

Figure 3. Continued

(E) Cell proliferation was assessed following activation of naive T cells with platebound TCR stimulation (1 $\mu\text{g}/\text{mL}$ αCD3) and the indicated concentration of αCD28 .

(F and G) Expression levels of ICOS and CTLA-4 was measured 72 h following platebound activation at the indicated αCD28 concentrations. Showing representative plots from 1 of 3 individual experiments. Data are represented as mean \pm SD. Statistical significance was determined using a two-way ANOVA with Šidák correction. * = $p < 0.05$, ** = $p < 0.01$, *** = $p < 0.001$.

Enhanced eIF4E activity increases T_{EFF} cell sensitivity to TCR and co-stimulatory signals

Concurrently with enhanced Th1 differentiation, we also observed a global increase in T cell activation in $\text{BP}^{-/-}$ T_{EFF} cells during lung infection. This led us to investigate whether differences in TCR signaling could be responsible for the Th1 skewing of $\text{BP}^{-/-}$ CD4^{+} T cells. Many studies have suggested a link between the strength of TCR signals and Th-subset differentiation, with strong antigen stimulation or lower thresholds for cell activation being shown to drive increased IFN γ production in CD4^{+} T_{EFF} cells.^{45–47} To investigate how increased eIF4E activity impacts the responsiveness to TCR, we FACS-isolated naive ($\text{Foxp3}^{-}\text{CD44}^{-}\text{CD62L}^{+}$) CD4^{+} T cells from $\text{BP}^{-/-}$ and WT mice and polyclonally TCR-activated them with titrated doses of plate-bound αCD3 in the presence of αCD28 co-stimulation. $\text{BP}^{-/-}$ T cells showed increased upregulation of CD25 at equivalent TCR signal strength, with differences in CD25 expression increasing with time following activation (Figure 3A). CD5 expression is correlated with the level of affinity of TCRs to the MHC-peptide complexes, and a good indicator of TCR signal strength.^{48,49} Following TCR stimulation, $\text{BP}^{-/-}$ T cells showed increased upregulation of CD5 expression compared to WT cells showing a greater response to equivalent αCD3 signals. Furthermore, $\text{BP}^{-/-}$ cells treated with low αCD3 concentrations (0.02 $\mu\text{g}/\text{mL}$), showed comparable CD5 expression to WT cells treated with 1 $\mu\text{g}/\text{mL}$ αCD3 indicating a more robust response to weaker TCR signals (Figure 3B). We then examined this increase in TCR activation by directly assessing the downstream effector molecules activated upon TCR activation. Naive $\text{BP}^{-/-}$ CD4^{+} T cells showed increased phosphorylation of AKT directly following TCR stimulation (Figure 3C). In addition, $\text{BP}^{-/-}$ T cells showed increased RPS6 phosphorylation, indicating greater engagement of the mTOR pathway shortly following TCR engagement (Figure 3D). In parallel, we also examined if this increase in T cell activation could be due to a reduced reliance of $\text{BP}^{-/-}$ T cells on co-stimulatory signals. The CD28 signaling cascade is a classic activator of the PI3K/AKT axis, necessary to activate mTOR and in turn phosphorylate the eIF4EBPs. $\text{BP}^{-/-}$ T_{EFF} cells activated in the absence, or low concentration of αCD28 showed increased proliferative responses compared to WT T_{EFF} cells (Figure 3E). This observation was corroborated by an increased upregulation of both ICOS and CTLA-4 following activation, indicating a more activated cell phenotype despite low levels of CD28 co-stimulation in $\text{BP}^{-/-}$ T cells (Figures 3F and 3G).^{50,51} Thus, increased eIF4E activity in $\text{BP}^{-/-}$ T cells reduced their threshold for TCR signals and enhanced T cell activation, predisposing cells to a skewing toward Th1 differentiation.

Lack of eIF4EBP1 and 2 rescues the immunosuppressive effect of mTOR inhibition

One of the canonical pathways triggered by the CD28 signaling cascade is the activation of the mTOR complex.^{52,53} This leads to the phosphorylation of eIF4EBPs and the subsequent release of eIF4E to act within the cell. mTOR activity has also been shown to be necessary for Th1 differentiation in CD4^{+} T cells.⁵⁴ To examine if the phosphorylation of eIF4EBPs by mTOR was necessary for the activation and differentiation of CD4^{+} T cells and could be responsible for the differences in activation observed, we cultured naive $\text{BP}^{-/-}$ and WT CD4^{+} T cells in the presence of rapamycin to block mTOR activity. $\text{BP}^{-/-}$ T cells displayed a resistance to the antiproliferative effect of rapamycin, with increased cell proliferation compared to WT cells at equivalent rapamycin concentrations (Figure 4A). This was accompanied by an increase in cytokine secretion in rapamycin-treated cells, with a higher proportion of $\text{BP}^{-/-}$ T cells secreting IFN γ (Figure 4B). To confirm that $\text{BP}^{-/-}$ T cells still possessed elevated mTOR activity despite the presence of rapamycin, we then examined the levels of phosphorylated RPS6 within $\text{BP}^{-/-}$ and WT T cells at the same time point post activation. As expected, a higher proportion of $\text{BP}^{-/-}$ T cells maintained phosphorylated RPS6 expression despite the presence of increasing concentrations of rapamycin (Figure 4C). Elevated levels of mTOR activity are known to drive the differentiation of Th1 cells, with mTOR inhibition impairing Th1 differentiation. As such, we asked if $\text{BP}^{-/-}$ CD4^{+} T cells would similarly be resistant to the rapamycin-mediated inhibition of Th1 differentiation. To this end, naive $\text{BP}^{-/-}$ and WT CD4^{+} T cells were polarized to a Th1 phenotype using IL-12 in the presence of increasing concentrations of rapamycin. While WT T cells showed a sharp reduction in IFN γ secretion following rapamycin treatment, $\text{BP}^{-/-}$ cells maintained their Th1 phenotype with robust IFN γ secretion (Figure 4D). These results indicated that eIF4E hyper-activity in $\text{BP}^{-/-}$ T cells

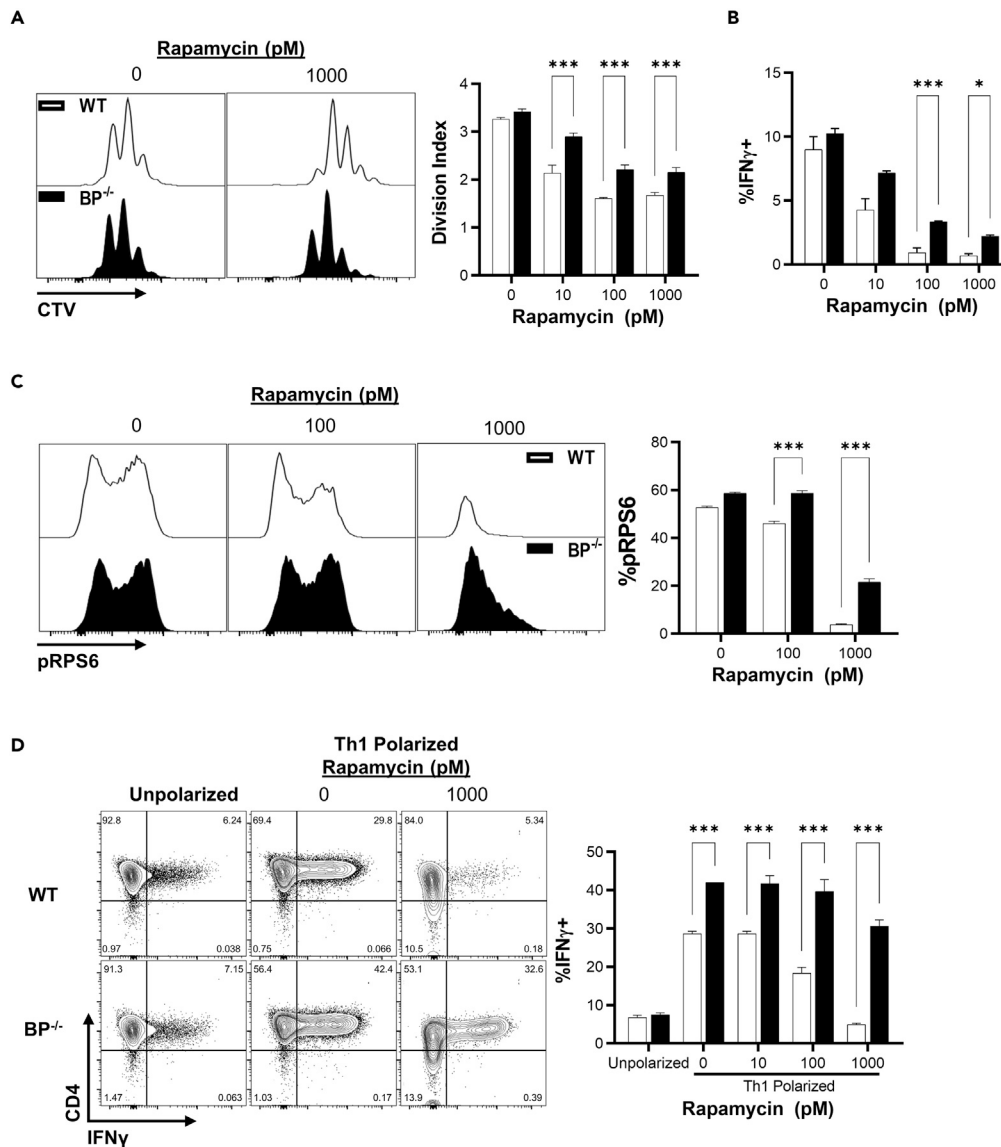


Figure 4. eIF4E-binding protein deficiency in T_{EFF} confers resistance to rapamycin-mediated immunosuppression

(A) CTV-labeled T_{EFF} cells were activated using platebound TCR stimulation for 72 h in media containing the indicated concentrations of rapamycin.

(B) Interferon gamma secretion was assessed in rapamycin-treated cells 72 h following activation.

(C) Analysis of phosphorylated RPS6 expression in T cells activated using platebound TCR stimulation for 72 h in media containing the indicated concentrations of rapamycin.

(D) T_{EFF} cells were polarized toward a Th1 phenotype using IL-12 (10 ng/mL) and treated with the indicated concentrations of rapamycin. All cytokine secretion data are from cells treated with PMA, Ionomycin, and Golgi-Stop for 3 h. Shown are representative plots from 1 of 3 individual experiments. Data are represented as mean \pm SD. Statistical significance was determined using a two-way ANOVA with Šidák correction. * = $p < 0.05$, ** = $p < 0.01$, *** = $p < 0.001$.

contributed the increases in T cell activation and Th1 polarization through activation of the mTOR-eIF4BP-eIF4E axis, potentially through the increased translation of eIF4E-sensitive mRNAs within T cells.

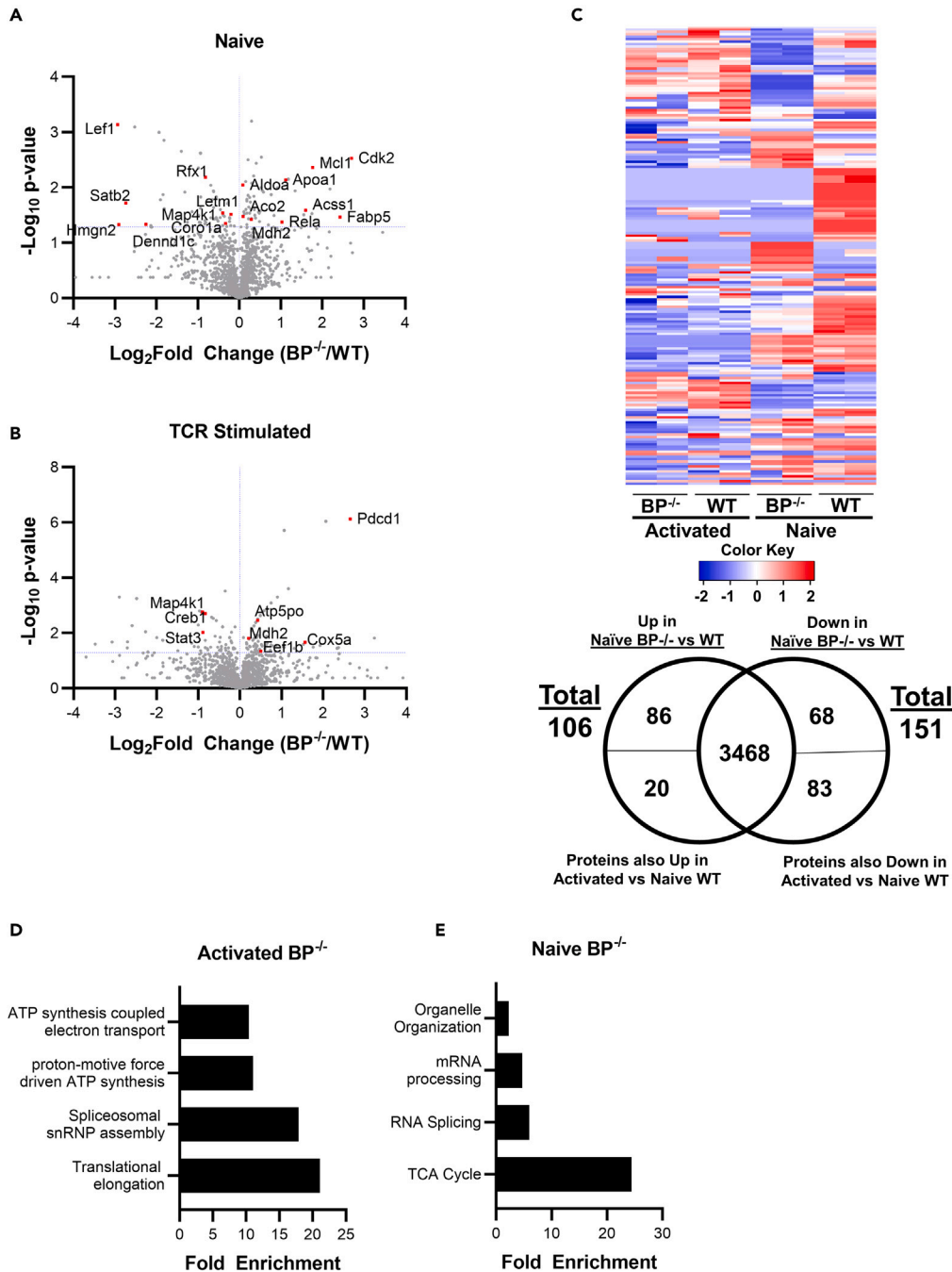
eIF4E hyper-activity in BP^{-/-} T_{EFF} cells facilitates the establishment of a proteome associated with cellular metabolism and proliferation

The ability of eIF4E to bind the 5' cap of mRNA is central to its role in the formation of the eIF4F complex for ribosome recruitment. Several studies have indicated that mRNAs associated with proliferation and cell

growth, including MCL-1 and BCL-2, are more sensitive to eIF4E levels.^{55–57} As such, we performed proteomic analysis of naive and TCR-activated BP^{-/-} and WT CD4⁺ T cells to examine how differences in baseline eIF4E activity could alter the proteome in resting (unstimulated) and TCR-activated states (Figures 5A and 5B) (A full list of differentially expressed proteins, along with raw spectrum counts can be found in Table S1). Relative to naive WT T cells, BP^{-/-} T cells showed increased expression of several proteins associated with cell proliferation, including MCL-1 and CDK2, while negative regulators of T cell activation, like Lef1 and Map4k1, were expressed at lower levels in BP^{-/-} naive T cells.^{58–61} Activated BP^{-/-} T_{EFF} cells also had increased expression of PD-1, corroborating our earlier observations in *Influenza A*-infected mice (Figure 1F). One possibility for the increased TCR sensitivity and activation of naive BP^{-/-} CD4⁺ T cells could be that eIF4E hyper-activity in naive T cells leads to the development of a proteome more akin to activated T_{EFF} cells, where mTOR activation following TCR and co-stimulation phosphorylates the eIF4EBPs releasing eIF4E to act within the cell. Comparison of the 257 differentially expressed proteins between naive BP^{-/-} and WT T_{EFF} cells with the 649 differentially expressed proteins distinguishing naive and activated WT T_{EFF} cells demonstrated that 103/257 differentially expressed proteins distinguishing naive BP^{-/-} from WT T_{EFF} cells had similar changes in expression as those found between naive and activated WT T_{EFF} cells (Figure 5C). Thus, the increased TCR sensitivity of BP^{-/-} CD4⁺ T cells could be due to the basal proteome of naive BP^{-/-} T cells containing elements found in activated T_{EFF} cells, enhancing their activation. We then examined the nature of the differentially expressed proteins by conducting overrepresentation analysis for biological processes associated with proteins expressed at higher levels in BP^{-/-} relative to WT T cells. Unsurprisingly, activated BP^{-/-} T_{EFF} cells showed an enrichment in proteins associated with mRNA translation (Figure 5D). However, activated BP^{-/-} T_{EFF} cells also showed an enrichment in proteins associated with cellular metabolism, the electron transport chain, and cellular respiration. In parallel, naive BP^{-/-} T cells showed enrichment in the citric acid cycle, indicating inherent differences in cellular metabolism in BP^{-/-} T cells (Figure 5E). This is of particular interest, as T cell metabolism is closely tied to their function. Altogether, it indicated that the basal proteome of naive BP T cells resulting from increased eIF4E activity is functionally distinct from that of WT T cells, in turn, impacting their ability to integrate T cell activation and differentiation signals.

Increased eIF4E activity renders T_{EFF} cells more metabolically active

The alterations in metabolic pathways uncovered in our proteomic analysis led us to investigate whether altered cellular metabolism could be responsible for the Th1 skewing of BP^{-/-} T_{EFF} cells. The importance of metabolism on T cell activation and differentiation has been extensively studied in recent years.^{62,63} High glycolytic activity has been implicated in Th1 cell differentiation, with increased glycolysis being shown to directly regulate increased production of IFN γ .^{64,65} IRF4 is an important regulator of T cell metabolism, responsible for promoting the expression of glycolytic enzymes to maintain high glycolytic activity following its induction by the activation of mTOR.^{66,67} BP^{-/-} T cells showed increased IRF4 expression, both in the presence and absence of co-stimulation, supporting the notion that enhanced glycolytic activity could be driving the increased activation and Th1 skewing of BP^{-/-} T cells (Figure 6A). As a proxy for measuring glycolytic activity, naive CD4⁺ T cells were activated for 48 h in the presence of a fluorescent glucose analog, 2-NBDG, to measure their glucose uptake.⁶⁸ BP^{-/-} T cells showed a significant increase in glucose uptake with increasing α CD3 and α CD28 stimulation compared to WT cells (Figure 6B and 6C). When these cells were treated with rapamycin, glucose uptake was decreased in both BP^{-/-} and WT cells; however, BP^{-/-} T cells continually maintained higher glucose uptake with increasing concentrations of rapamycin (Figure 6D). This increased glucose uptake by BP^{-/-} T cells further suggested that they could be undergoing higher levels of glycolysis. To examine the metabolic profile of BP^{-/-} T_{EFF} cells following TCR activation, we then conducted Seahorse extracellular flux analysis on naive CD4⁺ T cells activated with platebound α CD3 and α CD28 to obtain a measure of both glycolysis and cellular respiration 48 h following activation. Activated BP^{-/-} T cells showed a higher basal extracellular acidification rate, pointing to elevated metabolic activity. The extracellular acidification rate differences were further increased upon treatment of cells with oligomycin to block oxidative phosphorylation and enhance glycolytic activity, with BP^{-/-} T cells showing a higher glycolytic reserve (Figure 6E). Subsequent treatment of cells with BAM15, a mitochondrial uncoupler, revealed an increased oxygen consumption rate in BP^{-/-} T cells, indicating that BP^{-/-} T cells also possessed a higher capacity for oxidative phosphorylation. This increase in cellular metabolism was maintained with increasing TCR stimulus strength, as both glycolytic and mitochondrial ATP generation was elevated in BP^{-/-} T cells at both concentrations of α CD3 evaluated (Figure 6F). This increase in glycolytic ATP generation paralleled the differences in the polarization of naive BP^{-/-} T cells, with increased glycolytic activity being associated with Th1 differentiation. However, in the case of both iT_{REG} and Th17



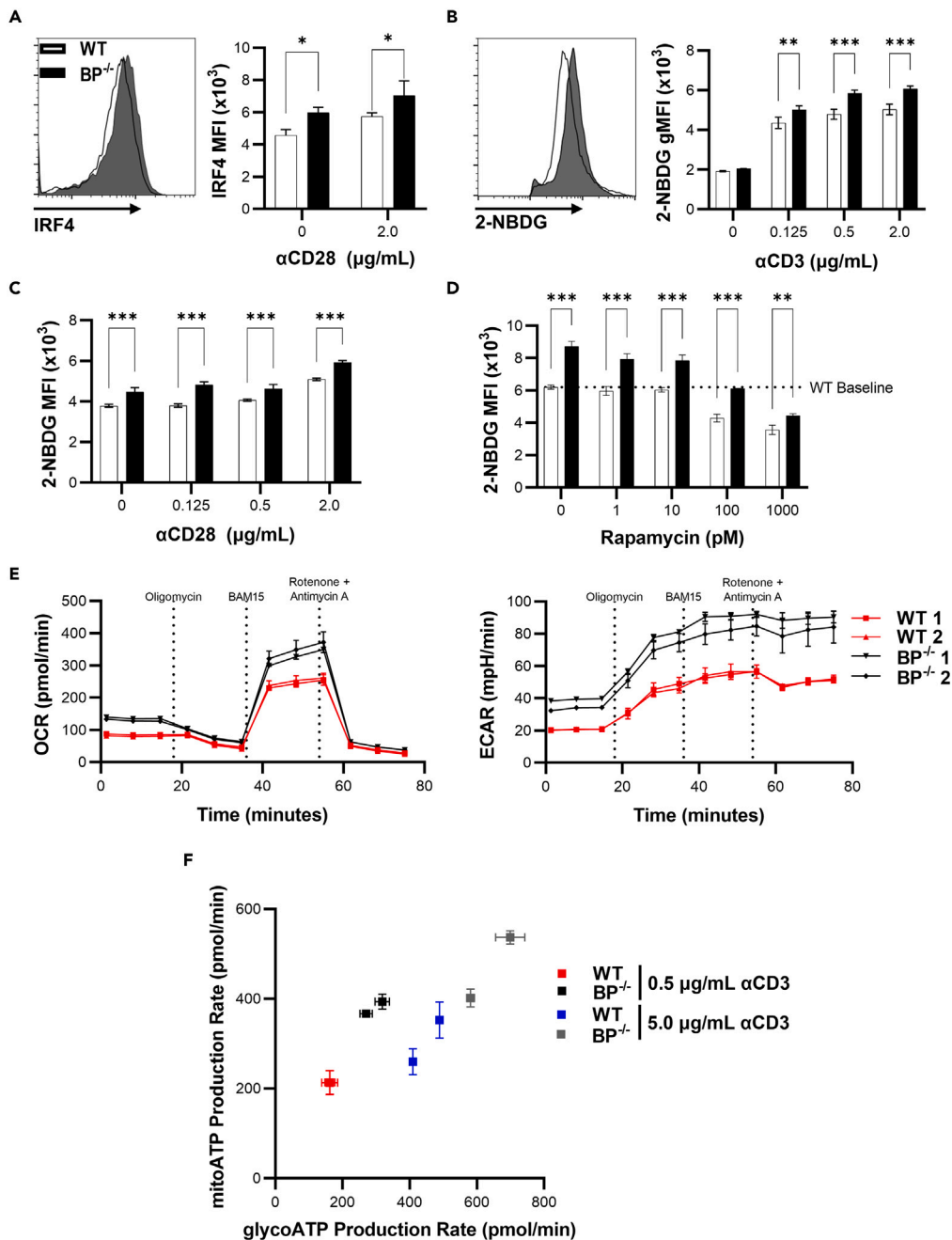


Figure 6. Increased eIF4E activity in BP^{-/-} T_{EFF} cells facilitates glucose uptake and metabolic activity following activation

(A) IRF4 expression was measured in T_{EFF} cells stimulated with platebound TCR with the presence or absence of α CD28. (B) Glucose uptake was measured in T_{EFF} cells at 48 h following platebound TCR stimulation at the indicated concentrations by culturing cells with 2-NBDG (75 μ M) for 30 min in glucose-free media. (C) Glucose uptake was measured in T_{EFF} cells at 48 h following platebound TCR stimulation with the indicated concentrations of α CD28 using 2-NBDG. (D) Glucose uptake was measured in T_{EFF} cells stimulated with platebound α CD3 and α CD28 in the presence of the indicated concentration of rapamycin using 2-NBDG at 48 h post stimulation.

Figure 6. Continued

(E) OCR and ECAR measurements from $BP^{-/-}$ and WT T_{EFF} activated for 48 h with platebound $\alpha CD3$ (0.5 $\mu g/mL$) and $\alpha CD28$ (2 $\mu g/mL$). Read using an Agilent Seahorse XFe96 using the T cell metabolic profiling kit. (Cells were isolated in 2 individual experiments prior to activation, both sets of cells were run in three technical replicates).

(F) Energetic Map of basal ATP production by $BP^{-/-}$ and WT T_{EFF} activated for 48 h with the indicated concentration of $\alpha CD3$. Energetic MAP was generated using the Agilent Seahorse Analytics platform from the basal ECAR and OCR rates detected for the appropriate sample. Showing representative plots from 1 of 3 individual experiments unless otherwise indicated. Data are represented as mean \pm SD. Statistical significance was determined using a two-way ANOVA with Sidak correction. * = $p < 0.05$, ** = $p < 0.01$, *** = $p < 0.001$.

differentiation, where oxidative phosphorylation is known to play a role in the induction and maintenance of these phenotypes, inhibition of oxidative phosphorylation via oligomycin resulted in a reduction in WT T cell polarization comparable to the reduced levels observed $BP^{-/-}$ T cells (Fig. S3A-B). Thus, although $BP^{-/-}$ T cells have increased cellular respiratory capacity and glycolytic activity, the relative contribution of glycolysis and oxidative phosphorylation is altered in $BP^{-/-}$ T cells resulting in their increased Th1 and decreased iTREG and Th17 polarization.

eIF4EBP1/2 deficiency in T cells specifically drives increased Th1 polarization during gut inflammation

We then examined how specific deletion of eIF4EBP1/2 in $CD4^{+}$ T cells would affect their function in an inflammatory setting *in vivo*. To this end, we made use of an adoptive transfer model, whereby FACS-isolated $BP^{-/-}$ and WT (Foxp3) T_{EFF} cells were co-injected (1:1 ratio) into T cell-deficient $TCR-\beta^{-/-}$ hosts and evaluated for their relative potential to undergo significant Th1 and Th17 polarization within the gut microenvironment, a prominent feature of this model. This allowed us to examine the role of eIF4EBP1/2 deficiency specifically in T_{EFF} cells, as both WT and $BP^{-/-}$ T_{EFF} cells were present in the same microenvironment and exposed to the same environmental signals. $BP^{-/-}$ T_{EFF} cells recovered from the spleen, mesenteric lymph nodes, and colon lamina propria showed increased levels of T cell activation, with greater proportions of CD25 expressing and actively cycling cells (Figures 7A and 7B). This increase in activation was accompanied by elevated expression of the co-stimulatory receptors PD-1, and CTLA-4, indicating a greater degree of T cell activation (Figures 7C and 7D). Examination of the Th1:Th17 balance showed that $BP^{-/-}$ T_{EFF} cells had higher secretion of $IFN\gamma$ while showing reduced IL-17A secretion (Figure 7E). This skewing to a Th1 phenotype was corroborated with an increase in the Th1 master transcription factor T-bet, and a decrease in RORyt expression (Figure 7F). Assessment of chemokine receptors also showed a preferential expression of Th1-associated CXCR3 over Th17-associated CCR6 in $BP^{-/-}$ T_{EFF} cells (Figure 7G). These results demonstrated that increased T cell-intrinsic eIF4E activity directly skewed $BP^{-/-}$ T cells toward a Th1 phenotype as WT T_{EFF} cells recovered from the same tissues, and consequently receiving the same polarizing signals, showed decreased Th1 differentiation while having increased Th17 differentiation.

While these differences were observed in T_{EFF} cells, we also examined the impact of eIF4EBP deficiency on T_{REG} cells using a similar adoptive transfer model and injecting purified WT and $BP^{-/-}$ T_{REG} cells (1:1 ratio) to determine if a similar skewing toward a Th1 phenotype would occur in $BP^{-/-}$ T_{REG} cells. This model is characterized by a loss of Foxp3 expression by T_{REG} cells in the gut microenvironment, generating pathogenic ex T_{REG} cells.⁶⁹ Although the defects in iTREG induction by $BP^{-/-}$ T_{EFF} (Figure 2C) cells would suggest that eIF4E hyper-activity would have a negative effect on Foxp3 expression, surprisingly, a higher proportion of donor $BP^{-/-}$ T_{REG} cells maintained expression of Foxp3 compared to co-transferred WT T_{REG} cells. (Figure S4A). Interestingly, among the cells that maintained Foxp3 expression, we observed increased CXCR3 expression which has been associated with T_{REG} cells adopting a Th1-like phenotype (Figure S4B).⁷⁰ We then further characterized this increased stability of Foxp3 expression using a T cell-mediated colitis model, whereby $BP^{-/-}$ or WT T_{REG} cells were co-transferred (1:4 ratio) with WT T_{EFF} cells into a lymphopenic host (Figure S4C). When cellular infiltration of the colon lamina propria was examined 21 days post T cell transfer, we observed a significant decrease in the number of infiltrating immune cells in the colons of mice receiving $BP^{-/-}$ T_{REG} cells compared to WT T_{REG} cells (Figure S4D). In accordance with our previous results, transferred $BP^{-/-}$ T_{REG} cells showed increased maintenance of Foxp3 expression (Figure S4E). Consequently, there was a reduction in the accumulation and proliferation of $CD45.1^{+}$ T_{EFF} cells in mice receiving $BP^{-/-}$ T_{REG} cells (Figure S4F and S4G). This was accompanied by a reduction in both Th1 and Th17 responses detected in $CD45.1^{+}$ T_{EFF} cells, due to the increased proportions of $CD45.2^{+}$ Foxp3 $^{+}$ $BP^{-/-}$ cells resulting in

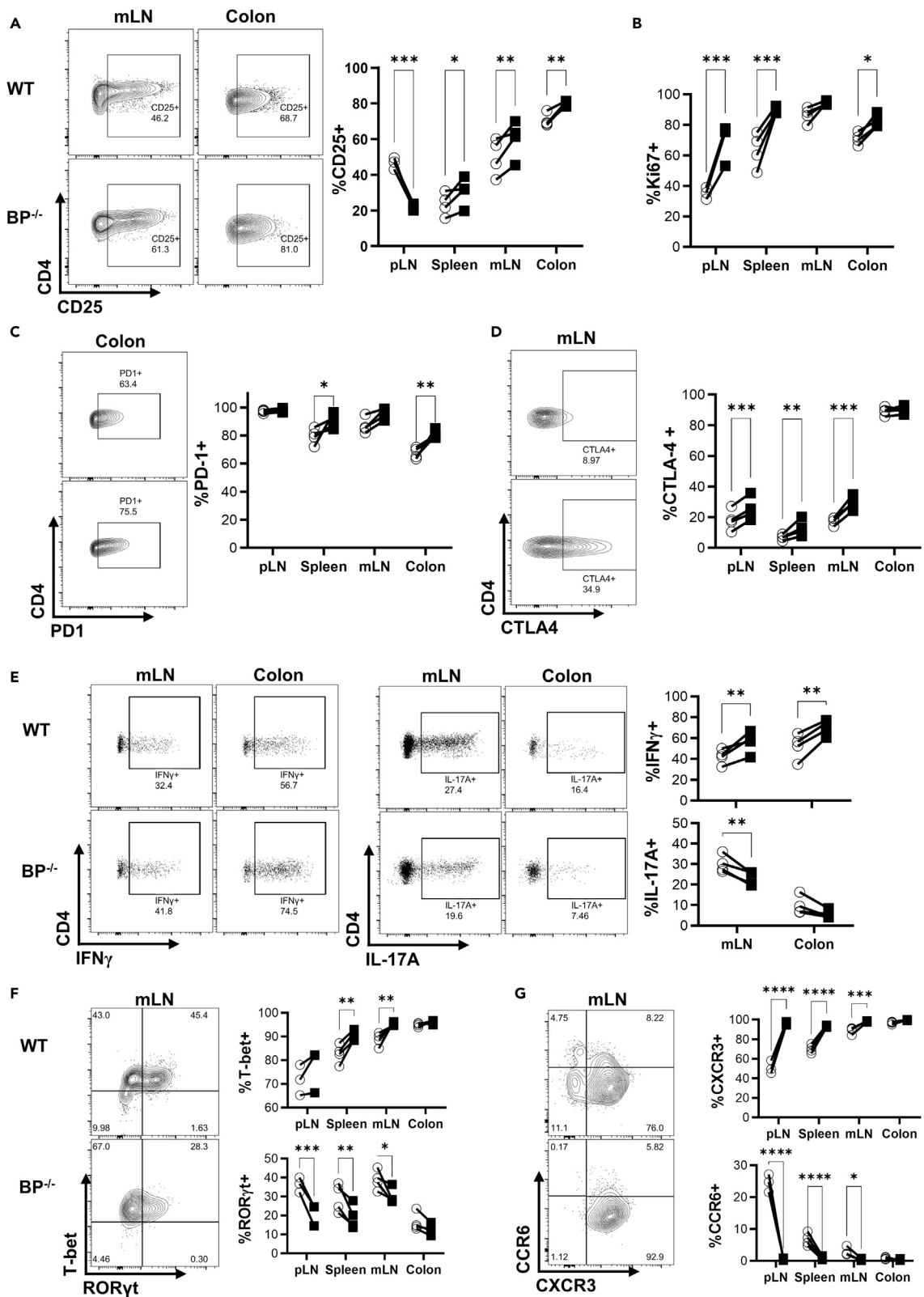


Figure 7. Increased eIF4E activity enhances Th1 differentiation while limiting Th17 differentiation during gut inflammation

Sorted CD45.1 WT and CD45.2 BP^{-/-} T_{EFF} cells were adoptively transferred into TCR- α -deficient hosts at a 1:1 ratio. Mice were sacrificed 14 days post injection. Showing 1 representative experiment of 3 individual repeats (n = 4–5). All flow plots are gated on viable CD4⁺ cells that are either CD45.1+ for WT plots or CD45.2+ for BP^{-/-} plots.

- (A) BP^{-/-} cells showed higher CD25 expression following adoptive transfer.
- (B) BP^{-/-} T_{EFF} cells had a higher proportion of actively proliferating cells compared to WT controls.
- (C and D) BP^{-/-} T_{EFF} shows higher levels of immune checkpoint expression (PD-1 and CTLA-4).
- (E) Interferon gamma and IL-17A secretion was assessed in BP^{-/-} and WT T_{EFF} cells following PMA/Ionomycin/Monensin treatment.
- (F) BP^{-/-} T_{EFF} showed decreased ROR γ t, and higher T-bet expression compared to WT controls.
- (G) BP^{-/-} T_{EFF} expressed higher levels of Th1-associated chemokine receptor CXCR3 compared to the Th17-associated chemokine receptor CCR6. All cytokine secretion data are from cells treated with PMA, Ionomycin, and Golgi-Stop for 3 h. Data are represented as mean \pm SD. Statistical significance was determined using a repeated measures two-way ANOVA with Šidák correction. * = p < 0.05, ** = p < 0.01, *** = p < 0.001.

increased control of gut inflammation (Figure S4H and S4I). Thus, although eIF4E drives Th1 polarization in T_{EFF} cells and the adoption of Th1-associated chemokine receptors by T_{REG} cells, its role in T cells is context dependent, with eIF4E-activity stabilizing Foxp3 expression in BP^{-/-} T_{REG} cells.

DISCUSSION

The adaptation and differentiation of CD4⁺ T cells is central to their ability to properly respond to a given immunological threat. This adaptation has been extensively studied revealing a complex network of signaling pathways and factors that give different Th-cell subsets their functions.^{3,71} Although the major driving factors behind the differentiation of Th-cell subsets have been defined, a growing body of evidence now shows how a variety of post-transcriptional processes can fine-tune T cell functions in response to different microenvironments.^{15,72} In line with this, our previously conducted genome-wide profiling of translational activity in T cells highlighted how different mRNA transcripts could be preferentially translated or suppressed following TCR stimulation in CD4⁺ T_{EFF} and T_{REG} cells.¹⁸ From this work, the differential translation of eIF4E mRNA drew our attention as eIF4E itself is a key regulator of global mRNA translation. Given the preferential translation of eIF4E mRNA in T_{EFF} cells, we sought to determine a potential role for eIF4E in T_{EFF} cells. Here, we show that the levels of eIF4E activity within CD4⁺ T cells can influence their differentiation, activation, and lineage commitment.

We first determined whether the level of eIF4E activity within T_{EFF} cells could directly affect their inflammatory capacity. Since eIF4E is essential for eukaryotic translation, we were not able to use a system causing complete eIF4E deficiency in murine cells. While others have conducted work on mice containing a deletion of one allele of eIF4E, it has been shown that a reduction in eIF4E expression results in a corresponding decrease in the expression of eIF4EBPs.⁷³ As such, it is thought that it is the ratio of eIF4EBP/eIF4E that influences eIF4E activity within a cell. Thus, we made use of eIF4EBP1 and 2-deficient mice (BP^{-/-}), where eIF4E would be hyper-active in T_{EFF} cells. Our findings in healthy, unchallenged mice revealed that this increase in eIF4E activity in BP^{-/-} T_{EFF} cells had a minimal functional impact on T_{EFF} cell activity under homeostatic conditions. This is in accordance with the fact that naive T_{EFF} cells are quiescent, showing minimal metabolic and inflammatory activity.⁷⁴ However, in the more immunologically active site within the colon lamina propria, we observed a specific skewing of BP^{-/-} T_{EFF} cells to a Th1 phenotype. This could be due to observations that TCR triggering of naive T_{EFF} cells could induce transient upregulation of T-bet expression, with the elevated eIF4E activity in BP^{-/-} mice cementing this transient Th1 profile into place.⁷⁵ This was further demonstrated using our low-dose *Influenza A* infection model where the milder phenotype associated with low-dose *Influenza A* infection was exacerbated in BP^{-/-} mice. This was evident in the increased weight-loss observed in BP^{-/-} mice, potentially due to the increased IFN γ secretion being found within the lungs, delaying the recovery period following infection. This led to the idea that increased eIF4E activity could just be exacerbating the typical immune response by T_{EFF} cells.

Our work then examined the notion that increased eIF4E activity acts as a feedforward loop on the polarizing signals received by T_{EFF} cells by polarizing them to different Th-cell lineages in isolation. Surprisingly, the effect of increased eIF4E activity in naive CD4⁺ T cells was limited to enhancing the Th1 differentiation. Although, BP^{-/-} T cells were still able to differentiate into Th2, Th17, and iT_{REG} cell lineages in the presence of the requisite polarizing cytokines, there was a reduction, rather than an amplification in their polarization. We further demonstrated that inhibition of eIF4E with

eIF4E-inhibitors was instead able to enhance iT_{REG} differentiation while suppressing the Th1 response. This is in line with other findings, that another inhibitor of eIF4E could enhance the differentiation of iT_{REG} cells.⁷⁶ This suggested that the level of eIF4E activity had a direct impact on the basal state of T cells, impacting their ability to surpass the initial Th1-like state following activation to commit to other Th cell lineages.

Aberrant eIF4E activity is known to directly impact cell proliferation in various cancer cell types.^{77,78} It is possible that the impact of eIF4E activity in $BP^{-/-}$ on T cell differentiation could be due to altered translation of mRNAs associated with T cell activation and proliferation. In line with this, our work shows that increases in eIF4E activity resulted in greater responses to TCR signals by $CD4^{+}$ T cells consistent with other studies showing alterations in TCR signaling strength driving altered T cell differentiation.⁷⁹ Surprisingly, this was also observed with co-stimulatory signals as $BP^{-/-}$ T cells were less reliant on CD28 signaling for their activation. These findings are in accordance with other studies showing that the activation of mTOR is necessary for the phosphorylation of eIF4EBPs, with CD28 signaling resulting in robust mTOR activation.⁸⁰ Thus, eIF4E may be required for the proper activation of $CD4^{+}$ T cells, with the mTOR-eIF4EBP-eIF4E axis facilitating protein synthesis to match the proliferative demands of recently activated T_{EFF} cells.

The essential role of mTOR in the activation and proliferation of T cells has been well established.⁸¹ Our finding that $BP^{-/-}$ T cells are resistant to the antiproliferative effects of rapamycin on T cells suggests that the phosphorylation of eIF4EBPs by mTOR is important to its function in T cells. This effect was further confirmed by examining a direct downstream effector of mTOR, RPS6, which showed that $BP^{-/-}$ T cells maintain higher phosphorylation of RPS6 despite the inhibitory effects of rapamycin. This also corroborates other findings that $BP^{-/-}$ B cells are resistant to the immunosuppressive effect of rapamycin.²⁹ Strikingly, we found that the absence of eIF4E-BP1/2 rendered T_{EFF} cells resistant to the impairment of Th1 differentiation by rapamycin. This further reinforces the idea that phosphorylation of eIF4EBPs by mTOR and subsequent release of eIF4E is necessary for the proper activation and effector function of T cells.

This study also evaluated the impact of increased eIF4E activity on the basal proteome of both naive and TCR-stimulated $CD4^{+}$ T cells. We found that the level of eIF4E activity within a T cell could directly regulate the translation and expression of genes associated with T cell activation. Surprisingly, we also found upregulation of genes associated with T cell metabolism. A finding that we further examined using metabolic profiling of T cells. We found that increased eIF4E activity rendered T_{EFF} cells more glycolytically active, showing increased glucose uptake following TCR stimulation, and increased maximal glycolytic activity as seen using a Seahorse extracellular flux analyzer. Our findings are in accordance with findings that the glucose transporter Glut 1 is preferentially translated in human T cells following activation,⁷⁶ indicating that the increased eIF4E activity in $BP^{-/-}$ T_{EFF} cells could be enhancing the translation of Glut1, among other metabolically associated mRNA transcripts, leading to increased glucose uptake and glycolytic activity, which in turn drives the skewing toward Th1 differentiation.

Furthermore, our current study builds on our previous work where we identified the eIF4E mRNA as being differentially translated between T_{REG} and T_{EFF} cells and demonstrated how increased eIF4E expression in T_{EFF} cells results in a corresponding increase in the expression of proliferation-associated genes.¹⁸ Furthermore, our study also compared the translational signature of activated T_{EFF} cells, where eIF4E was preferentially translated compared to activated T_{REG} cells, to the translational signature in cells obtained from the lungs of $BP^{-/-}$ and WT mice.⁸² This comparison highlighted strong similarities in the translational signatures differentiating activated T_{EFF} and T_{REG} cells and $BP^{-/-}$ and WT cells. This analysis confirms our results with $BP^{-/-}$ T cells displaying increased responses to TCR signals, and robust engagement of the Th1 differentiation pathway.

One limitation of our study is the use of mice that are globally deficient for eIF4EBPs making it difficult to examine the impact of increased eIF4E activity in T cells in isolation. We addressed this using our lymphopenic transfer experiments, where we could examine the impact of unrestricted eIF4E activity specifically in the T cell compartment, allowing for a direct comparison between WT and $BP^{-/-}$ T_{EFF} cells. These experiments reinforced our findings that the level of eIF4E activity within a T cell could impact their polarization capacity, driving Th1 polarization while limiting Th17 differentiation. Surprisingly, when we repeated these same transfer experiments using isolated T_{REG} cells, we saw an increased maintenance of Foxp3 in $BP^{-/-}$ T_{REG} cells. This stood in contrast to our previous observations that $BP^{-/-}$ T_{EFF} cells were less able to induce

Foxp3 in response to TGF- β which had suggested that increased eIF4E activity may have a destabilizing role in Foxp3 expression. One possible explanation for this observation is an increase in the translation of some eIF4E-sensitive mRNAs associated with cell survival or proliferation in BP^{-/-} T_{REG} cells, which would normally not occur in WT T_{REG} cells where the translation of eIF4E mRNA is repressed. Another possibility is an increase in the translation of Foxp3 mRNA preventing the action of any destabilizing microRNA, which is known to reduce the expression of Foxp3.⁸³ However, while it is unclear why BP^{-/-} T_{REG} cells display increased maintenance of Foxp3 *in vivo*, Zeng et al. have demonstrated the necessity of mTORC1 activity for the suppressive function of T_{REG} cells. Interestingly, the increased mTOR activity in BP^{-/-} T cells following TCR stimulation could potentially explain why BP^{-/-} T_{REG} cells suppressed T_{EFF} responses more efficiently than their WT counterparts in our T cell-mediated colitis transfer experiments.⁸⁴ Altogether, this indicates that the role of eIF4E within a cell is context dependent, potentially reinforcing the existing transcriptional landscape through continued translation of relevant mRNAs. This raises the possibility in T_{EFF} cells isolated from other genetically defined mouse strains that are prone to exacerbated Th2 responses, i.e., BALB/c, that eIF4E may reinforce a more Th2-dominant phenotype.

Due to its involvement in the development of several cancer cell types, the regulation of eIF4E activity has become a prominent avenue of investigation. This includes inhibitors that directly target the ability of eIF4E to bind to the 5' cap of mRNA (4Ei-1 and Bn7GMP) as well as those that impact the ability of eIF4E to interact with eIF4G, to inhibit translation initiation and inhibit growth in malignant cell lines.⁸⁵⁻⁸⁷ Given the role of eIF4E in promoting T cell activation and Th1 responses in CD4⁺ T cells, the same strategies used to target malignant cell growth could be turned toward targeting aberrant T cell responses. To our knowledge, there have not been any studies showing the impact of directly targeting eIF4E during autoimmunity, either in murine models or clinical trials. However, one indirect way of targeting eIF4E activity has been to inhibit mTOR activity using rapamycin and various analogs to prevent the phosphorylation of eIF4EBPs. Rapamycin is a known immunosuppressive agent and has shown efficacy in several models of autoimmunity and clinical trials.⁸⁸⁻⁹⁰ Our work suggests that this effect could be due in part to the inhibitive effect of rapamycin on lymphocyte translation, limiting their activation and inflammatory effector function.

In summary, we demonstrate that the level of eIF4E activity within a T cell directly influences their activation, differentiation, and effector functions. However, the factors driving the increased translation of eIF4E mRNA in T_{EFF} cells remain to be elucidated. While we have demonstrated the impact of increased eIF4E activity, further study of the regulation of eIF4E within T cells could provide insights for therapeutic interventions to modulate T cell plasticity and inflammation.

Limitations of the study

One limitation of this study, as previously discussed, is the use of mice globally deficient in eIF4E-BPs in our analysis of the BP^{-/-} phenotype both *ex vivo* and following challenge with *Influenza A*. It is possible that the T cell development could have been altered due to the lack of eIF4E-BPs in all cell types involved during lymphocyte development. Although we attempted to address this issue using adoptive transfer models to examine the impact of eIF4E-BP deficiency specifically in T cells, this model is not entirely analogous to physiological activity of T cells *in vivo* as T cell activation and proliferation in a lymphopenic setting could have influenced the role played by altered eIF4E activity in these experiments. As such, a CD4^{Cre}eif4ebp1^{fllox/fllox}eif4ebp2^{fllox/fllox} mouse model would have been beneficial to examine T cell-specific deletion of eIF4E-BPs directly *in vivo*. Our study would also benefit from an increased number of samples for the proteomic analysis of WT and BP^{-/-} T cells. Finally, although the proteomic analyses did highlight key differences in protein expression, this study would have benefited from transcriptome analysis of WT and BP^{-/-} T cells to conclusively show that the altered eIF4E activity level in BP^{-/-} T cells is directly impacting the translation of T cell-specific mRNA transcripts.

STAR★METHODS

Detailed methods are provided in the online version of this paper and include the following:

- [KEY RESOURCES TABLE](#)
- [RESOURCE AVAILABILITY](#)
 - Lead contact
 - Materials availability

- Data and code availability
- EXPERIMENTAL MODEL AND SUBJECT DETAILS
 - Mice
- METHOD DETAILS
 - Isolation of primary murine lymphocytes
 - CD4⁺ T cell isolation
 - *In vitro* T cell assays
 - Seahorse real time cell metabolic analysis
 - Proteomic analysis
 - Influenza infections
 - Adoptive transfer experiments
 - Flow cytometry
- QUANTIFICATION AND STATISTICAL ANALYSIS

SUPPLEMENTAL INFORMATION

Supplemental information can be found online at <https://doi.org/10.1016/j.isci.2023.106683>.

ACKNOWLEDGMENTS

This work was funded by a Canadian Institutes of Health Research (CIHR) operating grant (PJT-148821) awarded to C.A.P. We thank the RI-MUHC Immunophenotyping Platform for their excellent cell sorting service. We also thank the RI-MUHC Proteomics Platform for their help in the design and execution of the proteomic analyses.

AUTHOR CONTRIBUTIONS

Conceptualization: R.I. and C.A.P.; Investigation: R.I., T.A., and F.A.; Formal Analysis: R.I. and C.A.P.; Methodology: R.I., T.A., and F.A.; Writing – Original Draft: R.I. and C.A.P.; Writing – Review & Editing: R.I., T.A., F.A., and C.A.P.; Funding Acquisition: C.A.P.; Resources: J.A.S., C.W., and C.A.P.

DECLARATION OF INTERESTS

The authors declare no competing interests.

Received: July 29, 2022

Revised: February 27, 2023

Accepted: April 11, 2023

Published: April 18, 2023

REFERENCES

1. Perez-Riverol, Y., Bai, J., Bandla, C., García-Seisdedos, D., Hewapathirana, S., Kamatchinathan, S., Kundu, D.J., Prakash, A., Frericks-Zipper, A., Eisenacher, M., et al. (2022). The PRIDE database resources in 2022: a hub for mass spectrometry-based proteomics evidences. *Nucleic Acids Res.* 50, D543–D552. <https://doi.org/10.1093/nar/gkab1038>.
2. Korn, T., Bettelli, E., Oukka, M., and Kuchroo, V.K. (2009). IL-17 and Th17 cells. *Annu. Rev. Immunol.* 27, 485–517. <https://doi.org/10.1146/annurev.immunol.021908.132710>.
3. Zhou, L., Chong, M.M.W., and Littman, D.R. (2009). Plasticity of CD4⁺ T cell lineage differentiation. *Immunity* 30, 646–655. <https://doi.org/10.1016/j.immuni.2009.05.001>.
4. Bin Dhuban, K., Kornete, M., S Mason, E., and Piccirillo, C.A. (2014). Functional dynamics of Foxp3⁺ regulatory T cells in mice and humans. *Immunol. Rev.* 259, 140–158. <https://doi.org/10.1111/imr.12168>.
5. Brunkow, M.E., Jeffery, E.W., Hjerrild, K.A., Paepfer, B., Clark, L.B., Yasayko, S.-A., Wilkinson, J.E., Galas, D., Ziegler, S.F., and Ramsdell, F. (2001). Disruption of a new forkhead/winged-helix protein, scurfy, results in the fatal lymphoproliferative disorder of the scurfy mouse. *Nat. Genet.* 27, 68–73. <https://doi.org/10.1038/83784>.
6. Hori, S., Nomura, T., and Sakaguchi, S. (2003). Control of regulatory T cell development by the transcription factor Foxp3. *Science* 299, 1057–1061. <https://doi.org/10.1126/science.1079490>.
7. Sujino, T., London, M., Hoytema van Konijnenburg, D.P., Rendon, T., Buch, T., Silva, H.M., Lafaille, J.J., Reis, B.S., and Mucida, D. (2016). Tissue adaptation of regulatory and intraepithelial CD4⁺ T cells controls gut inflammation. *Science* 352, 1581–1586. <https://doi.org/10.1126/science.aaf3892>.
8. Miragaia, R.J., Gomes, T., Chomka, A., Jardine, L., Riedel, A., Hegazy, A.N., Whibley, N., Tucci, A., Chen, X., Lindeman, I., et al. (2019). Single-cell transcriptomics of regulatory T cells reveals trajectories of tissue adaptation. *Immunity* 50, 493–504.e7. <https://doi.org/10.1016/j.immuni.2019.01.001>.
9. Dumitru, C., Kabat, A.M., and Maloy, K.J. (2018). Metabolic adaptations of CD4⁺ T cells in inflammatory disease. *Front. Immunol.* 9, 540. <https://doi.org/10.3389/fimmu.2018.00540>.
10. Boothby, I.C., Cohen, J.N., and Rosenblum, M.D. (2020). Regulatory T cells in skin injury: at the crossroads of tolerance and tissue repair. *Sci. Immunol.* 5, eaaz9631. <https://doi.org/10.1126/sciimmunol.aaz9631>.
11. Arpaia, N., Green, J.A., Moltedo, B., Arvey, A., Hemmers, S., Yuan, S., Treuting, P.M., and

- Rudensky, A.Y. (2015). A distinct function of regulatory T cells in tissue protection. *Cell* 162, 1078–1089. <https://doi.org/10.1016/j.cell.2015.08.021>.
12. Ravindran, R., and McSorley, S.J. (2005). Tracking the dynamics of T-cell activation in response to Salmonella infection. *Immunology* 114, 450–458. <https://doi.org/10.1111/j.1365-2567.2005.02140.x>.
 13. Vogel, C., and Marcotte, E.M. (2012). Insights into the regulation of protein abundance from proteomic and transcriptomic analyses. *Nat. Rev. Genet.* 13, 227–232.
 14. Persson, O., Brynne, U., Levander, F., Widegren, B., Salford, L.G., and Krogh, M. (2009). Proteomic expression analysis and comparison of protein and mRNA expression profiles in human malignant gliomas. *Proteomics. Clin. Appl.* 3, 83–94.
 15. Istomine, R., Pavey, N., and Piccirillo, C.A. (2016). Posttranscriptional and translational control of gene regulation in CD4⁺ T cell subsets. *J. Immunol.* 196, 533–540. <https://doi.org/10.4049/jimmunol.1501337>.
 16. Mazumder, B., Li, X., and Barik, S. (2010). Translation control: a multifaceted regulator of inflammatory response. *J. Immunol.* 184, 3311–3319. <https://doi.org/10.4049/jimmunol.0903778>.
 17. Carpenter, S., Ricci, E.P., Mercier, B.C., Moore, M.J., and Fitzgerald, K.A. (2014). Post-transcriptional regulation of gene expression in innate immunity. *Nat. Rev. Immunol.* 14, 361–376. <https://doi.org/10.1038/nri3682>.
 18. Bjur, E., Larsson, O., Yurchenko, E., Zheng, L., Gandin, V., Topisirovic, I., Li, S., Wagner, C.R., Sonenberg, N., and Piccirillo, C.A. (2013). Distinct translational control in CD4⁺ T cell subsets. *PLoS Genet.* 9, e1003494. <https://doi.org/10.1371/journal.pgen.1003494>.
 19. Mamane, Y., Petroulakis, E., Rong, L., Yoshida, K., Ler, L.W., and Sonenberg, N. (2004). eIF4E – from translation to transformation. *Oncogene* 23, 3172–3179. <https://doi.org/10.1038/sj.onc.1207549>.
 20. Crew, J.P., O'Brien, T.S., and Harris, A.L. (1996). Bladder cancer angiogenesis, its role in recurrence, stage progression and as a therapeutic target. *Cancer Metastasis Rev.* 15, 221–230.
 21. Pettersson, F., Yau, C., Dobocan, M.C., Culjkovic-Kraljicic, B., Retrouvey, H., Puckett, R., Flores, L.M., Krop, I.E., Rousseau, C., Cocolakis, E., et al. (2011). Ribavirin treatment effects on breast cancers overexpressing eIF4E, a biomarker with prognostic specificity for luminal B-type breast Cancer: eIF4E as a target and a prognostic marker in breast cancer. *Clin. Cancer Res.* 17, 2874–2884.
 22. Matthews-Greer, J., Caldito, G., de Benedetti, A., Herrera, G.A., Dominguez-Malagon, H., Chanona-Vilchis, J., and Turbat-Herrera, E.A. (2005). eIF4E as a marker for cervical neoplasia. *Appl. Immunohistochem. Mol. Morphol.* 13, 367–370.
 23. Culjkovic, B., and Borden, K.L. (2009). Understanding and targeting the eukaryotic translation initiation factor eIF4E in head and neck cancer. *J. Oncol.* 2009, 981679. <https://doi.org/10.1016/j.jco.2009.08.004>.
 24. Topisirovic, I., Guzman, M.L., McConnell, M.J., Licht, J.D., Culjkovic, B., Neering, S.J., Jordan, C.T., and Borden, K.L.B. (2003). Aberrant eukaryotic translation initiation factor 4E-dependent mRNA transport impedes hematopoietic differentiation and contributes to leukemogenesis. *Mol. Cell Biol.* 23, 8992–9002.
 25. Richter, J.D., and Sonenberg, N. (2005). Regulation of cap-dependent translation by eIF4E inhibitory proteins. *Nature* 433, 477–480. <https://doi.org/10.1038/nature03205>.
 26. Raught, B., and Gingras, A.-C. (1999). eIF4E activity is regulated at multiple levels. *Int. J. Biochem. Cell Biol.* 31, 43–57. [https://doi.org/10.1016/S1357-2725\(98\)00131-9](https://doi.org/10.1016/S1357-2725(98)00131-9).
 27. Peter, D., Igreja, C., Weber, R., Wohlbold, L., Weiler, C., Ebertsch, L., Weichenrieder, O., and Izaurralde, E. (2015). Molecular architecture of 4E-BP translational inhibitors bound to eIF4E. *Mol. Cell* 57, 1074–1087. <https://doi.org/10.1016/j.molcel.2015.03.020>.
 28. Mader, S., Lee, H., Pause, A., and Sonenberg, N. (1995). The translation initiation factor eIF-4E binds to a common motif shared by the translation factor eIF-4 gamma and the translational repressors 4E-binding proteins. *Mol. Cell Biol.* 15, 4990–4997.
 29. So, L., Lee, J., Palafox, M., Mallya, S., Woxland, C.G., Arguello, M., Truitt, M.L., Sonenberg, N., Ruggiero, D., and Fruman, D.A. (2016). The 4E-BP-eIF4E axis promotes rapamycin-sensitive growth and proliferation in lymphocytes. *Sci. Signal.* 9, ra57. <https://doi.org/10.1126/scisignal.aad8463>.
 30. Gingras, A.C., Gygi, S.P., Raught, B., Polakiewicz, R.D., Abraham, R.T., Hoekstra, M.F., Aebersold, R., and Sonenberg, N. (1999). Regulation of 4E-BP1 phosphorylation: a novel two-step mechanism. *Genes Dev.* 13, 1422–1437. <https://doi.org/10.1101/gad.13.11.1422>.
 31. Sukarieh, R., Sonenberg, N., and Pelletier, J. (2009). The eIF4E-binding proteins are modifiers of cytoplasmic eIF4E relocalization during the heat shock response. *Am. J. Physiol. Cell Physiol.* 296, C1207–C1217. <https://doi.org/10.1152/ajpcell.00448.2009>.
 32. Pons, B., Peg, V., Vázquez-Sánchez, M.A., López-Vicente, L., Argelaguet, E., Coch, L., Martínez, A., Hernández-Losa, J., Armengol, G., and Ramon y Cajal, S. (2011). The effect of p-4E-BP1 and p-eIF4E on cell proliferation in a breast cancer model. *Int. J. Oncol.* 39, 1337–1345.
 33. Pause, A., Belsham, G.J., Gingras, A.-C., Donzé, O., Lin, T.-A., Lawrence, J.C., and Sonenberg, N. (1994). Insulin-dependent stimulation of protein synthesis by phosphorylation of a regulator of 5'-cap function. *Nature* 371, 762–767. <https://doi.org/10.1038/371762a0>.
 34. Yanagiya, A., Suyama, E., Adachi, H., Svitkin, Y.V., Aza-Blanc, P., Imataka, H., Mikami, S., Martineau, Y., Ronai, Z.A., and Sonenberg, N. (2012). Translational homeostasis via the mRNA cap-binding protein, eIF4E. *Mol. Cell* 46, 847–858. <https://doi.org/10.1016/j.molcel.2012.04.004>.
 35. Müller, D., Lasfargues, C., El Khawand, S., Alard, A., Schneider, R.J., Bousquet, C., Pyronnet, S., and Martineau, Y. (2013). 4E-BP restrains eIF4E phosphorylation. *Translation* 1, e25819. <https://doi.org/10.4161/tra.25819>.
 36. Romagnoli, A., D'Agostino, M., Ardiccioni, C., Maracci, C., Motta, S., La Teana, A., and Di Marino, D. (2021). Control of the eIF4E activity: structural insights and pharmacological implications. *Cell. Mol. Life Sci.* 78, 6869–6885. <https://doi.org/10.1007/s00018-021-03938-z>.
 37. Martineau, Y., Azar, R., Bousquet, C., and Pyronnet, S. (2013). Anti-oncogenic potential of the eIF4E-binding proteins. *Oncogene* 32, 671–677. <https://doi.org/10.1038/nc.2012.116>.
 38. Hufford, M.M., Kim, T.S., Sun, J., and Braciale, T.J. (2015). The effector T cell response to influenza infection. *Curr. Top. Microbiol. Immunol.* 386, 423–455. https://doi.org/10.1007/82_2014_397.
 39. Lawrence, C.W., Ream, R.M., and Braciale, T.J. (2005). Frequency, specificity, and sites of expansion of CD8⁺ T cells during primary pulmonary influenza virus infection. *J. Immunol.* 174, 5332–5340. <https://doi.org/10.1093/infdis/jim100>.
 40. Rygiel, T.P., Rijkers, E.S.K., de Ruiter, T., Stolte, E.H., van der Valk, M., Rimmelzwaan, G.F., Boon, L., van Loon, A.M., Coenjaerts, F.E., Hoek, R.M., et al. (2009). Lack of CD200 enhances pathological T cell responses during influenza infection. *J. Immunol.* 183, 1990–1996. <https://doi.org/10.4049/jimmunol.0900252>.
 41. Moskopidid, D., and Kiousis, D. (1998). Contribution of virus-specific CD8⁺ cytotoxic T cells to virus clearance or pathologic manifestations of influenza virus infection in a T cell receptor transgenic mouse model. *J. Exp. Med.* 188, 223–232. <https://doi.org/10.1084/jem.188.2.223>.
 42. Liu, A.N., Mohammed, A.Z., Rice, W.R., Fiedelvey, D.T., Liebermann, J.S., Whitsett, J.A., Braciale, T.J., and Enelow, R.I. (1999). Perforin-independent CD8⁺ T-cell-mediated cytotoxicity of alveolar epithelial cells is preferentially mediated by tumor necrosis factor- α . *Am. J. Respir. Cell Mol. Biol.* 20, 849–858. <https://doi.org/10.1165/ajrcmb.20.5.3585>.
 43. Shveygert, M., Kaiser, C., Bradrick, S.S., and Gromeier, M. (2010). Regulation of eukaryotic translation initiation factor 4E (eIF4E) phosphorylation by mitogen-activated protein kinase occurs through modulation of Mnk1-eIF4G interaction. *Mol. Cell Biol.* 30, 5160–5167. <https://doi.org/10.1128/mcb.00448-10>.
 44. Webster, K.R., Goel, V.K., Hung, I.N., Parker, G.S., Staunton, J., Neal, M., Molter, J., Chiang, G.G., Jessen, K.A., Wegerski, C.J., et al. (2015). eFT508, a potent and selective mitogen-activated protein kinase interacting kinase (MNK) 1 and 2 inhibitor, is efficacious in preclinical models of diffuse large B-cell lymphoma (DLBCL). *Blood* 126, 1554. <https://doi.org/10.1182/blood.V126.23.1554.1554>.

45. Constant, S., Pfeiffer, C., Woodard, A., Pasqualini, T., and Bottomly, K. (1995). Extent of T cell receptor ligation can determine the functional differentiation of naive CD4+ T cells. *J. Exp. Med.* *182*, 1591–1596.
46. Ise, W., Totsuka, M., Sogawa, Y., Ametani, A., Hachimura, S., Sato, T., Kumagai, Y., Habu, S., and Kaminogawa, S. (2002). Naive CD4+ T cells exhibit distinct expression patterns of cytokines and cell surface molecules on their primary responses to varying doses of antigen. *J. Immunol.* *168*, 3242–3250.
47. Pfeiffer, C., Stein, J., Southwood, S., Ketelaar, H., Sette, A., and Bottomly, K. (1995). Altered peptide ligands can control CD4 T lymphocyte differentiation in vivo. *J. Exp. Med.* *181*, 1569–1574.
48. Azzam, H.S., Grinberg, A., Lui, K., Shen, H., Shores, E.W., and Love, P.E. (1998). CD5 expression is developmentally regulated by T cell receptor (TCR) signals and TCR avidity. *J. Exp. Med.* *188*, 2301–2311.
49. Persaud, S.P., Parker, C.R., Lo, W.-L., Weber, K.S., and Allen, P.M. (2014). Intrinsic CD4+ T cell sensitivity and response to a pathogen are set and sustained by avidity for thymic and peripheral complexes of self peptide and MHC. *Nat. Immunol.* *15*, 266–274. <https://doi.org/10.1038/ni.2822>.
50. Dong, C., Juedes, A.E., Temann, U.-A., Shresta, S., Allison, J.P., Ruddle, N.H., and Flavell, R.A. (2001). ICOS co-stimulatory receptor is essential for T-cell activation and function. *Nature* *409*, 97–101. <https://doi.org/10.1038/35051100>.
51. Walunas, T.L., Bakker, C.Y., and Bluestone, J.A. (1996). CTLA-4 ligation blocks CD28-dependent T cell activation. *J. Exp. Med.* *183*, 2541–2550. <https://doi.org/10.1084/jem.183.6.2541>.
52. Colombetti, S., Basso, V., Mueller, D.L., and Mondino, A. (2006). Prolonged TCR/CD28 engagement drives IL-2-independent T cell clonal expansion through signaling mediated by the mammalian target of rapamycin. *J. Immunol.* *176*, 2730–2738.
53. Zheng, Y., Collins, S.L., Lutz, M.A., Allen, A.N., Kole, T.P., Zarek, P.E., and Powell, J.D. (2007). A role for mammalian target of rapamycin in regulating T cell activation versus anergy. *J. Immunol.* *178*, 2163–2170.
54. Delgoffe, G.M., Polizzi, K.N., Waickman, A.T., Heikamp, E., Meyers, D.J., Horton, M.R., Xiao, B., Worley, P.F., and Powell, J.D. (2011). The kinase mTOR regulates the differentiation of helper T cells through the selective activation of signaling by mTORC1 and mTORC2. *Nat. Immunol.* *12*, 295–303. <https://doi.org/10.1038/ni.2005>.
55. Sonenberg, N., and Gingras, A.-C. (1998). The mRNA 5' cap-binding protein eIF4E and control of cell growth. *Curr. Opin. Cell Biol.* *10*, 268–275.
56. Rousseau, D., Kaspar, R., Rosenwald, I., Gehrke, L., and Sonenberg, N. (1996). Translation initiation of ornithine decarboxylase and nucleocytoplasmic transport of cyclin D1 mRNA are increased in cells overexpressing eukaryotic initiation factor 4E. *Proc. Natl. Acad. Sci. USA* *93*, 1065–1070.
57. Bhat, M., Robichaud, N., Hulea, L., Sonenberg, N., Pelletier, J., and Topisirovic, I. (2015). Targeting the translation machinery in cancer. *Nat. Rev. Drug Discov.* *14*, 261–278.
58. Chunder, N., Wang, L., Chen, C., Hancock, W.W., and Wells, A.D. (2012). Cyclin-dependent kinase 2 controls peripheral immune tolerance. *J. Immunol.* *189*, 5659–5666.
59. Faia, K., Toso, A., Fetalvero, K., Roche, M., Bench, S., O'Hearn, E., Cao, Q., Bright, K.-A., Paduraru, D., Romagnani, A., et al. (2021). MAP4K1 inhibition enhances immune cell activation and anti-tumor immunity in preclinical tumor models. *Cancer Res.* *81*, 1717.
60. Xing, S., Gai, K., Li, X., Shao, P., Zeng, Z., Zhao, X., Zhao, X., Chen, X., Paradee, W.J., Meyerholz, D.K., et al. (2019). Tcf1 and Lef1 are required for the immunosuppressive function of regulatory T cells. *J. Exp. Med.* *216*, 847–866. <https://doi.org/10.1084/jem.20182010>.
61. Tripathi, P., Koss, B., Opferman, J.T., and Hildeman, D.A. (2013). Mcl-1 antagonizes Bax/Bak to promote effector CD4+ and CD8+ T-cell responses. *Cell Death Differ.* *20*, 998–1007. <https://doi.org/10.1038/cdd.2013.25>.
62. Rangel Rivera, G.O., Knochenmann, H.M., Dwyer, C.J., Smith, A.S., Wyatt, M.M., Rivera-Reyes, A.M., Thaxton, J.E., and Paulos, C.M. (2021). Fundamentals of T Cell metabolism and strategies to enhance cancer immunotherapy. *Front. Immunol.* *12*, 645242. <https://doi.org/10.3389/fimmu.2021.645242>.
63. Buck, M.D., O'Sullivan, D., and Pearce, E.L. (2015). T cell metabolism drives immunity. *J. Exp. Med.* *212*, 1345–1360. <https://doi.org/10.1084/jem.20151159>.
64. Chang, C.H., Curtis, J.D., Maggi, L.B., Jr., Faubert, B., Villarino, A.V., O'Sullivan, D., Huang, S.C.C., van der Windt, G.J.W., Blagih, J., Qiu, J., et al. (2013). Posttranscriptional control of T cell effector function by aerobic glycolysis. *Cell* *153*, 1239–1251. <https://doi.org/10.1016/j.cell.2013.05.016>.
65. Peng, M., Yin, N., Chhangawala, S., Xu, K., Leslie, C.S., and Li, M.O. (2016). Aerobic glycolysis promotes T helper 1 cell differentiation through an epigenetic mechanism. *Science* *354*, 481–484. <https://doi.org/10.1126/science.aaf6284>.
66. Man, K., Miasari, M., Shi, W., Xin, A., Henstridge, D.C., Preston, S., Pellegrini, M., Belz, G.T., Smyth, G.K., Febbraio, M.A., et al. (2013). The transcription factor IRF4 is essential for TCR affinity-mediated metabolic programming and clonal expansion of T cells. *Nat. Immunol.* *14*, 1155–1165. <https://doi.org/10.1038/ni.2710>.
67. Mahnke, J., Schumacher, V., Ahrens, S., Käding, N., Feldhoff, L.M., Huber, M., Rupp, J., Raczkowski, F., and Mittrücker, H.W. (2016). Interferon Regulatory Factor 4 controls TH1 cell effector function and metabolism. *Sci. Rep.* *6*, 35521. <https://doi.org/10.1038/srep35521>.
68. Zou, C., Wang, Y., and Shen, Z. (2005). 2-NBDG as a fluorescent indicator for direct glucose uptake measurement. *J. Biochem. Biophys. Methods* *64*, 207–215. <https://doi.org/10.1016/j.jbbm.2005.08.001>.
69. Zhou, X., Bailey-Bucktrout, S.L., Jeker, L.T., Penaranda, C., Martínez-Llordella, M., Ashby, M., Nakayama, M., Rosenthal, W., and Bluestone, J.A. (2009). Instability of the transcription factor Foxp3 leads to the generation of pathogenic memory T cells in vivo. *Nat. Immunol.* *10*, 1000–1007. <https://doi.org/10.1038/ni.1774>.
70. Kitz, A., and Dominguez-Villar, M. (2017). Molecular mechanisms underlying Th1-like Treg generation and function. *Cell. Mol. Life Sci.* *74*, 4059–4075. <https://doi.org/10.1007/s00018-017-2569-y>.
71. Luckheeram, R.V., Zhou, R., Verma, A.D., and Xia, B. (2012). CD4+ T cells: differentiation and functions. *Clin. Dev. Immunol.* *2012*, 925135. <https://doi.org/10.1155/2012/925135>.
72. Jurgens, A.P., Popović, B., and Wolkers, M.C. (2021). T cells at work: how post-transcriptional mechanisms control T cell homeostasis and activation. *Eur. J. Immunol.* *51*, 2178–2187. <https://doi.org/10.1002/eji.202049055>.
73. Yanagiya, A., Suyama, E., Adachi, H., Svitkin, Y.V., Aza-Blanc, P., Imataka, H., Mikami, S., Martineau, Y., Ronai, Z.A., and Sonenberg, N. (2012). Translational homeostasis via the mRNA cap-binding protein. *Mol. Cell* *46*, 847–858. <https://doi.org/10.1016/j.molcel.2012.04.004>.
74. Yang, K., and Chi, H. (2018). Investigating cellular quiescence of T lymphocytes and antigen-induced exit from quiescence. *Methods Mol. Biol.* *1686*, 161–172. https://doi.org/10.1007/978-1-4939-7371-2_12.
75. Ariga, H., Shimohakamada, Y., Nakada, M., Tokunaga, T., Kikuchi, T., Kariyone, A., Tamura, T., and Takatsu, K. (2007). Instruction of naive CD4+ T-cell fate to T-bet expression and T helper 1 development: roles of T-cell receptor-mediated signals. *Immunology* *122*, 210–221. <https://doi.org/10.1111/j.1365-2567.2007.02630.x>.
76. Ricciardi, S., Manfrini, N., Alfieri, R., Calamita, P., Crosti, M.C., Gallo, S., Müller, R., Pagani, M., Abbrignani, S., and Biffo, S. (2018). The translational machinery of human CD4+ T cells is poised for activation and controls the switch from quiescence to metabolic remodeling. *Cell Metab.* *28*, 895–906.e5. <https://doi.org/10.1016/j.cmet.2018.08.009>.
77. Wan, J., Shi, F., Xu, Z., and Zhao, M. (2015). Knockdown of eIF4E suppresses cell proliferation, invasion and enhances cisplatin cytotoxicity in human ovarian cancer cells. *Int. J. Oncol.* *47*, 2217–2225. <https://doi.org/10.3892/ijo.2015.3201>.
78. Truitt, M.L., Conn, C.S., Shi, Z., Pang, X., Tokuyasu, T., Coady, A.M., Seo, Y., Barna, M., and Ruggero, D. (2015). Differential

- requirements for eIF4E dose in normal development and cancer. *Cell* 162, 59–71. <https://doi.org/10.1016/j.cell.2015.05.049>.
79. Snook, J.P., Kim, C., and Williams, M.A. (2018). TCR signal strength controls the differentiation of CD4(+) effector and memory T cells. *Sci. Immunol.* 3, eaas9103. <https://doi.org/10.1126/sciimmunol.aas9103>.
80. Chi, H. (2012). Regulation and function of mTOR signalling in T cell fate decisions. *Nat. Rev. Immunol.* 12, 325–338. <https://doi.org/10.1038/nri3198>.
81. Waickman, A.T., and Powell, J.D. (2012). mTOR, metabolism, and the regulation of T-cell differentiation and function. *Immunol. Rev.* 249, 43–58. <https://doi.org/10.1111/j.1600-065X.2012.01152.x>.
82. Kim, Y.Y., Linda, V.W., Ola, L., Danhua, F., Jon, M.U., Mark, S.P., Stephen, S.H., Vitaly, A.P., and Peter, B.B. (2009). Eukaryotic initiation factor 4E binding protein family of proteins: sentinels at a translational control checkpoint in lung tumor defense. *Cancer Res.* 69, 8455–8462.
83. Liu, C., Li, N., and Liu, G. (2020). The role of MicroRNAs in regulatory T cells. *J. Immunol. Res.* 2020, 3232061. <https://doi.org/10.1155/2020/3232061>.
84. Zeng, H., Yang, K., Cloer, C., Neale, G., Vogel, P., and Chi, H. (2013). mTORC1 couples immune signals and metabolic programming to establish T(reg)-cell function. *Nature* 499, 485–490. <https://doi.org/10.1038/nature12297>.
85. Li, S., Sun, C., Teng, N., Yang, W., Zhou, L., Zhang, Y., and Wagner, C.R. (2013). Treatment of breast and lung cancer cells with a N-7 benzyl guanosine monophosphate tryptamine phosphoramidate pronucleotide (4Ei-1) results in chemosensitization to gemcitabine and induced eIF4E proteasomal degradation. *Protein Eng. Des. Sel.* 26, 523–531.
86. Jia, Y., Chiu, T.-L., Amin, E.A., Polunovsky, V., Bitterman, P.B., and Wagner, C.R. (2010). Design, synthesis and evaluation of analogs of initiation factor 4E (eIF4E) cap-binding antagonist Bn7-GMP. *Eur. J. Med. Chem.* 45, 1304–1313. <https://doi.org/10.1016/j.ejmech.2009.11.054>.
87. Papadopoulos, E., Jenni, S., Kabha, E., Takroui, K.J., Yi, T., Salvi, N., Luna, R.E., Gavathiotis, E., Mahalingam, P., Arthanari, H., et al. (2014). Structure of the eukaryotic translation initiation factor eIF4E in complex with 4EGI-1 reveals an allosteric mechanism for dissociating eIF4G. *Proc. Natl. Acad. Sci. USA* 111, E3187–E3195. <https://doi.org/10.1073/pnas.1410250111>.
88. Bagherpour, B., Salehi, M., Jafari, R., Bagheri, A., Kiani-Esfahani, A., Edalati, M., Kardi, M.T., and Shaygannejad, V. (2018). Promising effect of rapamycin on multiple sclerosis. *Mult. Scler. Relat. Disord.* 26, 40–45. <https://doi.org/10.1016/j.msard.2018.08.009>.
89. Teachey, D.T., Obzut, D.A., Axsom, K., Choi, J.K., Goldsmith, K.C., Hall, J., Hulitt, J., Manno, C.S., Maris, J.M., Rhodin, N., et al. (2006). Rapamycin improves lymphoproliferative disease in murine autoimmune lymphoproliferative syndrome (ALPS). *Blood* 108, 1965–1971. <https://doi.org/10.1182/blood-2006-01-010124>.
90. Bride, K.L., Vincent, T., Smith-Whitley, K., Lambert, M.P., Bleesing, J.J., Seif, A.E., Manno, C.S., Casper, J., Grupp, S.A., and Teachey, D.T. (2016). Sirolimus is effective in relapsed/refractory autoimmune cytopenias: results of a prospective multi-institutional trial. *Blood* 127, 17–28. <https://doi.org/10.1182/blood-2015-07-657981>.
91. Alvarez, F., Istomine, R., Shourian, M., Pavey, N., Al-Aubodah, T.A.-F., Qureshi, S., Fritz, J.H., and Piccirillo, C.A. (2019). The alarmins IL-1 and IL-33 differentially regulate the functional specialisation of Foxp3+ regulatory T cells during mucosal inflammation. *Mucosal Immunol.* 12, 746–760. <https://doi.org/10.1038/s41385-019-0153-5>.
92. Hodgins, B., Yam, K.K., Winter, K., Pillet, S., Landry, N., and Ward, B.J. (2017). A single intramuscular dose of a plant-made virus-like particle vaccine elicits a balanced humoral and cellular response and protects young and aged mice from influenza H1N1 virus challenge despite a modest/absent humoral response. *Clin. Vaccine Immunol.* 24, e00273-17. <https://doi.org/10.1128/cvi.00273-17>.

STAR★METHODS

KEY RESOURCES TABLE

REAGENT or RESOURCE	SOURCE	IDENTIFIER
Antibodies		
Anti-mouse CD4 Alexa Fluor 700	Thermo Fisher	Clone: GK1.5, Cat #56-0041-82; RRID:AB_493999
Anti-mouse CD4 eFluor 450	Thermo Fisher	Clone: GK1.5, Cat #48-0041-82; RRID:AB_10718983
Anti-mouse CD44 APC	BD Biosciences	Clone: IM7, Cat # 561862; RRID:AB_10897144
Anti-mouse CD62L PercpCy5.5	Thermo Fisher	Clone: MEL-14, Cat # 45-0621-82; RRID:AB_996667
Anti-mouse Foxp3 FITC	Thermo Fisher	Clone: FJK-16s, Cat # 11-5773-82; RRID:AB_465243
Anti-mouse ICOS PE	BD Biosciences	Clone: 7E.17G9, Cat # 552146; RRID:AB_394349
Anti-mouse CTLA4 PeCy7	Biogend	Clone: UC10-4B9, Cat # 106314; RRID:AB_2564238
Anti-mouse IL-4 PE	BD Biosciences	Clone: 11B11, Cat # 554435; RRID:AB_395391
Anti-mouse CD25 PercpCy5.5	Thermo Fisher	Clone: PC61.5, Cat # 45-0251-82; RRID:AB_914324
Anti-mouse ICOS APC	Thermo Fisher	Clone:C398.4A, Cat # 17-9949-80; RRID:AB_11149500
Anti-mouse CD3 BUV 737	BD Biosciences	Clone: 17A2, Cat # 612803; RRID:AB_2870130
Anti-mouse PD1 PE	Thermo Fisher	Clone: J43, Cat # 12-9985-82; RRID:AB_466295
Anti-mouse/human phospho-AKT1 Pe	Thermo Fisher	Clone: SDRNR, Cat # 12-9715-41; RRID:AB_2637098
Anti-mouse IFN gamma PeCy7	Thermo Fisher	Clone XMG1.2, Cat # 25-7311-82; RRID:AB_469680
Anti-mouse IFN gamma APC	BD Biosciences	Clone: XMG 1.2, Cat #554413; RRID:AB_398551
Anti-mouse IL-2 APC	BD Biosciences	Clone: JES6-5H4, Cat # 554429; RRID:AB_398555
Anti-mouse phospho STAT3	Thermo Fisher	Clone: LUVNKLA, Cat # 17-9033-41; RRID:AB_2573281
Anti-mouse IRF4 eFluor660	Thermo Fisher	Clone: 3E4, Cat # 50-9858-82; RRID:AB_2574393
Anti-mouse CD25 APC	Thermo Fisher	Clone: PC61.5, Cat #17-0251-82; RRID:AB_469366
Anti-mouse IFN gamma BUV737	BD Biosciences	Clone XMG1.2, Cat #612769; RRID:AB_2870098
Anti-mouse/human T-bet PeCy7	Thermo Fisher	Clone: eBio4510, Cat # 25-5825-82; RRID:AB_11042699
Anti-mouse/human ROR gamma t PE	Thermo Fisher	Clone: AFKJS-9, Cat # 12-6988-82; RRID:AB_1834470
Anti-mouse GATA3 BUV395	BD Biosciences	Clone: L50-823, Cat# 565448; RRID:AB_2739241
Anti-mouse Ki-67 BUV395	BD Biosciences	Clone: B56, Cat # 564071; RRID:AB_2738577
Anti-mouse IL-17A APC	Thermo Fisher	Clone eBio17B7, Cat # 17-7177-81; RRID:AB_763580
Anti-mouse PD1 PeCy7	Thermo Fisher	Clone: J43, Cat # 25-9985-82; RRID:AB_10853805
Anti-mouse CD45.1 ApcCy7	BD Biosciences	Clone: A20, Cat # 560579; RRID:AB_1727487
Anti-mouse CD45.2 ApcCy7	BD Biosciences	Clone: 104, Cat # 560694; RRID:AB_1727492
Anti-mouse CXCR3 APC	Thermo Fisher	Clone CXCR3-173, Cat # 17-1831-82; RRID:AB_1210791
Anti-mouse CD5 APC/Fire750	Biogend	Clone: 53-7.3, Cat # 100634; RRID:AB_2687000
Anti-mouse ROR gamma t BV786	BD Biosciences	Clone: Q31-378, Cat # 564723; RRID:AB_2738916
Anti-mouse CCR6 BV421	BD Biosciences	Clone: 140706, Cat # 564736; RRID:AB_2738926
Anti-mouse Ki67 V450	BD Biosciences	Clone: B56, Cat # 561281; RRID:AB_10613816
Anti-mouse phospho RPS6	Biogend	Clone: A18024A, Cat # 93570; RRID:AB_2892494
Anti mouse phospho STAT4	Thermo Fisher	Clone: 4LURPIE, Cat # 12-9904-42; RRID:AB_2572689
Anti-mouse CD3e Purified	Thermo Fisher	Cat #16-0031-86; RRID:AB_468849
Anti-mouse CD28 Purified	Thermo Fisher	Cat #16-0281-86; RRID:AB_468923

(Continued on next page)

Continued

REAGENT or RESOURCE	SOURCE	IDENTIFIER
Chemicals, Peptides, and Recombinant Proteins		
Recombinant mouse IL-12p70	Peprotech	Cat #210-12
Recombinant mouse IL-4	BioLegend	Cat #574302
Recombinant mouse IL-6	BioLegend	Cat #575704
Recombinant mouse TGF-B1	Biologend	Cat #763104
Phorbol 12-myristate 13-acetate	Sigma-Aldrich	Cat #P1585
Ionomycin calcium salt	Sigma-Aldrich	Cat #I0634
BD Golgi Stop Protein Transport Inhibitor	BD Biosciences	Cat #554724
Mitomycin C	Sigma-Aldrich	Cat #M4287
EDTA	Thermo Fisher	Cat #15575-038
Collagenase IV	Sigma-Aldrich	Cat #11088866001
Critical Commercial Assays		
Fixable Viability Dye eFluor 780	Thermo Fisher	Cat # 65-0865-14
Fixable Viability Dye eFluor 506	Thermo Fisher	Cat # 65-0866-18
CD4 (L3T4) Microbeads	Miltenyi Biotec	Cat #130-117-043
Foxp3/Transcription Factor Fixation/Permeabilization Kit	Thermo Fisher	Cat # 00-5521-00
Permeabilization Buffer 10X	Thermo Fisher	Cat # 00-8333-56
Cell Trace Violet Cell Proliferation Kit	Thermo Fisher	Cat #C34571
2-NBDG	Thermo Fisher	Cat #N13195
Seahorse XF T cell metabolic profiling kit	Agilent	Cat # 103772-100
Deposited Data		
Proteomics Data	https://www.ebi.ac.uk/pride/	Accession: PXD039635 https://doi.org/10.6019/PXD039635
Experimental Models: Organisms/Strains		
Mouse: C57BL/6 Foxp3 ^{GFP}	Laboratory of Dr. Alexander Rudensky	N/A
Mouse: C57BL/6 Foxp3 ^{GFP} Eif4ebp1 ^{-/-} Eif4ebp2 ^{-/-}	Bred in house from Eif4ebp1 ^{-/-} Eif4ebp2 ^{-/-} provided by Dr. Nahum Sonnenberg	N/A
Mouse: C57BL/6-Foxp3 ^{GFP-CRE-ERT2}	The laboratory of Dr. Woong-Kyung Suh	N/A
Mouse: C57BL/6-Foxp3 ^{GFP-CRE-ERT2} Eif4ebp1 ^{-/-} Eif4ebp2 ^{-/-}	Bred in house from Eif4ebp1 ^{-/-} Eif4ebp2 ^{-/-} provided by Dr. Nahum Sonnenberg	N/A
Mouse: C57BL/6 Ly5.1+ TCRb ^{-/-}	Jackson Laboratory	B6.129P2-Tcrbtm1Mom/J Stock No.002118
Software and Algorithms		
FlowJo	BD Biosciences	https://www.flowjo.com/
GraphPad Prism	GraphPad Software	https://www.graphpad.com/scientific-software/prism/
Scaffold Viewer	Proteome Software	https://www.proteomesoftware.com/products

RESOURCE AVAILABILITY

Lead contact

Further information and requests for resources and reagents should be directed to and will be fulfilled by the lead contact, Ciriaco A. Piccirillo (ciro.piccirillo@mcgill.ca).

Materials availability

This study did not generate new unique reagents.

Data and code availability

The mass spectrometry proteomics data have been deposited to the ProteomeXchange Consortium via the PRIDE¹ partner repository with the dataset identifier PRIDE: PXD039635 and 10.6019/PXD039635. This paper does not report original code. Any additional information required to reanalyze the data reported in this paper is available from the [lead contact](#) upon request.

EXPERIMENTAL MODEL AND SUBJECT DETAILS

Mice

C57BL/6-Eif4ebp1^{-/-}Eif4ebp2^{-/-} mice were kindly provided by Dr. Nahum Sonenberg (McGill University, Canada), C57BL/6-Foxp3^{GFP} knock-in mice were kindly provided by Dr. Alexander Rudensky (Memorial Sloan Kettering Cancer Centre, NY) and C57BL/6-Foxp3^{GFP-CRE-ERT2} mice were kindly provided by Dr. Woong-Kyung Suh (McGill University, Canada). Mice were bred in house to generate C57BL/6-Foxp3^{GFP}Eif4ebp1^{-/-}Eif4ebp2^{-/-} and C57BL/6-Foxp3^{GFP-CRE-ERT2}Eif4ebp1^{-/-}Eif4ebp2^{-/-} mice. C57BL/6 TCRβ^{-/-} mice were purchased from Jackson Laboratories. All mice were bred and housed under specific pathogen-free conditions and used in accordance with McGill University's animal research practices. All experiments were conducted using age (8-12 weeks) and sex-matched littermates.

METHOD DETAILS

Isolation of primary murine lymphocytes

For the *in vitro* T cell polarization and activation assays, lymphocytes were isolated from peripheral lymph nodes and spleens through mechanical dissociation followed by red blood cell lysis using ACK lysis buffer for 30 seconds. For isolation of lung cells, lungs were minced into small pieces and incubated in HBSS containing 1mg/mL Collagenase IV and 0.1 mg/mL DNase I for 45 minutes. Incubated lung pieces were then mashed through a 70 μM filter, followed by red blood cell lysis using ACK lysis buffer. Isolation of cells from the colon lamina propria was conducted as previously described.⁹¹ Colons were flushed using 1X PBS and cut longitudinally and cut into 1cm segments. These segments were then washed in HBSS containing 5mM EDTA for 30 min. Segments were then washed and incubated in cRPMI containing 1mg/mL collagenase IV and 100 ng/mL DNase for 1 hour at 37°C in a rotating rack to liberate cells. All cell preparations were then filtered through 70 μM nylon mesh filters to obtain single cell suspensions that could be used for staining or further processing.

CD4⁺ T cell isolation

For the *in vitro* T cell and adoptive transfer assays T_{EFF} were isolated from C57BL/6-Foxp3^{GFP} and C57BL/6-Foxp3^{GFP}Eif4ebp1^{-/-}Eif4ebp2^{-/-} mice. Pooled lymph node and spleen cells were stained with mouse CD4 microbeads (Miltenyi Biotec) as per manufacturer s.o.p and then positively selected using a Miltenyi AutoMACS. Enriched CD4⁺ cells were then stained with CD4-AF700 and CD4⁺Foxp3^{GFP}- T_{EFF} cells were purified using a BD FACSAria Fusion cell sorter (>99% Purity). For naive cell isolation, used in the T cell polarization and activation assays and proteomic analysis, CD4⁺ T cells were also stained with CD62L-PerCP-Cy5.5 and CD44-APC during cell sorting to obtain Naive CD44⁺CD62L⁺ T_{EFF} cells (>99% purity).

In vitro T cell assays

For T Cell polarization assays, FACS-isolated naive CD4⁺ T cells were cultured in RPMI-1640 (Wisent) supplemented with 10% FBS (Wisent), 1% sodium pyruvate (Wisent), 1% 1 M Hepes (Wisent), 1% MEM nonessential amino acids (Wisent) and 1% 10,000 U/mL penicillin-streptomycin (Gibco). For iT_{REG} induction cells (1*10⁵) were activated using platebound αCD3(5μg/mL) and αCD28 (2μg/mL) (BD Biosciences) and cultured for 72 hours at 37°C in the presence of TGFβ (Novoprotein). For Th2, Th17 and Th1 polarization cells (5*10⁴) were activated using soluble αCD3(1μg/mL) and mitomycin-C (Sigma-Aldrich) treated

antigen-presenting cells in the presence of IL-4 (Biolegend), TGF- β and IL-6 (Biolegend), or IL-12 (Pepro-
tech) respectively. For T cell activation assays, naive CD4⁺ T cells were labeled with CellTrace Violet pro-
liferation dye (ThermoFisher) according to manufacturer s.o.p and activated using platebound α CD3
and α CD28 at the indicated concentration and collected at the indicated time points post activation.
For glucose uptake assays, naive T_{EFF} cells were activated for 48 hours prior to collection in glucose free
medium. After 2 washes, cells were then incubated in the presence of 75 μ M 2-NBDG (ThermoFisher) for
30 min at 37°C prior to being collected for flow cytometric analysis. For experiments involving rapamycin,
rapamycin (Sigma-Aldrich) was added at the point of T cell activation at the indicated concentrations.

Seahorse real time cell metabolic analysis

Metabolic analysis of naive T_{EFF} cells was conducted using the Seahorse XF T cell Metabolic Profiling Kit
(Agilent). FACS isolated naive T_{EFF} cells were activated using platebound α CD3 and α CD28 for 48 hours
prior to being collected for the assay. Cell preparation was conducted according to the manufacturer's in-
structions provided with the kit. Prepared samples were run using a Seahorse XFe96 analyzer (Agilent).
Data was analyzed using Agilent's Seahorse Analytics platform.

Proteomic analysis

Total protein was isolated directly from FACS isolated naive T_{EFF} cells or following 48 hours of platebound
 α CD3 and α CD28 stimulation. Protein extraction was conducted using RIPA lysis buffer containing anti-
phosphatases (Roche). Mouse lysate samples were then loaded onto a single stacking gel band to remove
lipids, detergents and salts. The single gel band containing all proteins was reduced with DTT, alkylated
with iodoacetic acid and digested with trypsin. 2 μ g of extracted peptides were re-solubilized in 0.1%
aqueous formic acid and loaded onto a Thermo Acclaim Pepmap (Thermo, 75 μ M ID X 2cm C18 3 μ M beads)
precolumn and then onto an Acclaim Pepmap Easyspray (Thermo, 75 μ M X 15cm with 2 μ M C18 beads)
analytical column separation using a Dionex Ultimate 3000 uHPLC at 250 nl/min with a gradient of 2-
35% organic (0.1% formic acid in acetonitrile) over 3 hours. Peptides were analyzed using a Thermo Orbi-
trap Fusion mass spectrometer operating at 120,000 resolution (FWHM in MS1) with HCD sequencing
(15,000 resolution) at top speed for all peptides with a charge of 2+ or greater. The raw data were converted
into *.mgf format (Mascot generic format) for searching using the Mascot 2.6.2 search engine (Matrix Sci-
ence) against Mouse Uniprot sequences (2020). The database search results were loaded onto Scaffold Q+
Scaffold_4.9.0 (Proteome Sciences) for statistical treatment and data visualization. Data points were
normalized to total spectrum counts along with imputing a minimum value of 0.5. These normalized values
were then used in the comparison between BP^{-/-} and WT naive T cells as well asl between BP^{-/-} and WT acti-
vated T cells via Student's t test. Raw spectrum counts and normalized values with expression changes for
both naive and activated T cells can be found in [Table S1](#). The mass spectrometry proteomics data have
been deposited to the ProteomeXchange Consortium via the PRIDE¹ partner repository with the dataset
identifier PRIDE: PXD039635 and 10.6019/PXD039635.

Influenza infections

Wild-type A/California/07/2009H1N1 virus was obtained from the National Microbiology Laboratory, Pub-
lic Health Agency of Canada. Virs was propagated using a Madin-Darby canine kidney cell line (American
Type Culture collection no PTA-6503). The 50% lethality dose (LD₅₀) was determined using titration exper-
iments previously conducted by Hodgins et al.⁹² In brief, groups of 8-week-old WT C57BL/6 mice were in-
fected with various multiples of TCID₅₀ of wild-type A/California/07/2009H1N1 by intranasal instillation,
and weight loss was monitored daily for 12 days. The LD₅₀ was found to be ~663 TCID₅₀. The C57BL/
6_{-F_{oxp3}GFP-CRE-ERT2} and C57BL/6_{-F_{oxp3}GFP-CRE-ERT2}Eif4ebp1^{-/-}Eif4ebp2^{-/-} were anesthetized with Isoflurane
prior to intranasal instillation (25 μ L/nare, 50 μ L total) to challenge mice with a sublethal 1/4 LD₅₀ dose of
H1N1. Mice were monitored daily for weight loss.

Adoptive transfer experiments

For adoptive transfer experiments, FACS-isolated T_{EFF} cells from CD45.1+ C57BL/6-Foxp3^{GFP} and
CD45.2+C57BL/6-Foxp3^{GFP}Eif4ebp1^{-/-}Eif4ebp2^{-/-} mice were intravenously injected (1:1 ratio, 5*10⁵ per
cell type) into CD45.1+ C57BL/6 TCR β ^{-/-} mice. Adoptive transfers were left for 14 days to allow for the ho-
meostatic proliferation of injected cells. Peripheral lymph nodes, spleens mesenteric lymph nodes and
spleens were collected from mice following euthanasia and processed as described earlier.

Flow cytometry

For all experiments containing cytokine secretion data, cells were incubated for 3 hours at 37°C with PMA, Ionomycin (Sigma-Aldrich) and monensin (BD Golgi Stop™) prior to collection for flow cytometry. Upon cell collection, single cell suspensions were stained with fixable viability dye eFluor506 or eFluor780 (ThermoFisher) in PBS according to manufacturer's s.o.p. Extracellular marker staining was carried out in PBS using monoclonal antibodies with directly conjugated fluorochromes. A full list of all antibodies used can be found in the [key resources table](#). Cells were then fixed using the eBioscience Fcγ3/transcription factor staining kit according to manufacturer s.o.p. (ThermoFisher). Intracellular staining was conducted in permeabilization buffer provided with the kit (ThermoFisher) using monoclonal antibodies with directly conjugated fluorochromes. Samples were acquired using a BD LSRFortessa X-20 flow cytometer (BD Biosciences). Data was analysed using FlowJo software (Version 10) (BD Biosciences).

QUANTIFICATION AND STATISTICAL ANALYSIS

Statistical analyses were performed using GraphPad Prism, version 9 (GraphPad Software). All data are displayed as mean \pm standard deviation. Statistical significance was determined by unpaired Student's t test for comparisons of 2 groups and by one-way ANOVA with multiple comparisons and Dunnett Correction for analysis containing more than 2 groups. Multivariable comparisons containing multiple groups were evaluated using a two-way ANOVA multiple comparisons and Sidak's correction. P value of ≤ 0.05 was considered significant. P values were indicated on graphs as * $p \leq 0.05$, ** $p \leq 0.01$, *** $p \leq 0.001$.